

Proximal Methods for Sparse Optimal Scoring and Discriminant Analysis

Summer Atkins¹, Gudmundur Einarsson², Brendan Ames³, and Line Clemmensen⁴

¹Department of Mathematics, University of Florida, PO Box 118105, Gainesville, FL 32611-8105, srnatkins@ufl.edu

²deCODE Genetics, gudmundur.einarsson2@decode.is

³Department of Mathematics, University of Alabama, Box 870350, Tuscaloosa, AL 35487-0350, bpames@ua.edu

⁴Department of Applied Mathematics and Computer Science, Technical University of Denmark, Building 324, 2800 Kongens Lyngby, Denmark, lkhc@dtu.dk

December 14, 2024

Abstract

Linear discriminant analysis (LDA) is a classical method for dimensionality reduction, where discriminant vectors are sought to project data to a lower dimensional space for optimal separability of classes. Several recent papers have outlined strategies, based on exploiting sparsity of the discriminant vectors, for performing LDA in the high-dimensional setting where the number of features exceeds the number of observations in the data. However, many of these proposed methods lack scalable methods for solution of the underlying optimization problems. We consider an optimization scheme for solving the sparse optimal scoring formulation of LDA based on block coordinate descent. Each iteration of this algorithm requires update of a scoring vector, which admits an analytic formula, and update of the corresponding discriminant vector, which requires solution of a convex subproblem; we will propose several variants of this algorithm where the proximal gradient method or the alternating direction method of multipliers is used to solve this subproblem. We show that the per-iteration cost of these methods scales linearly in the dimension of the data provided restricted regularization terms are employed, and cubically in the dimension of the data in the worst case. Furthermore, we establish that when this block coordinate descent framework generates convergent subsequences of iterates, then these subsequences converge to the stationary points of the sparse optimal scoring problem. We demonstrate the effectiveness of our new methods with empirical results for classification of Gaussian data and data sets drawn from benchmarking repositories, including time-series and multispectral X-ray data, and provide `Matlab` and `R` implementations of our optimization schemes.

1 Introduction

Sparse discriminant techniques have become popular in the last decade due to their ability to provide increased interpretation as well as predictive performance for high-dimensional problems where few observations are present. These approaches typically build upon successes from sparse linear regression, in particular the LASSO and its variants (see [22, Section 3.4.2] and [23]), by augmenting existing schemes for linear discriminant analysis (LDA) with sparsity-inducing regularization terms, such as the ℓ_1 -norm and elastic net.

Thus far, little focus has been put on the optimization strategies of these sparse discriminant methods, nor their computational cost. We propose three novel optimization strategies to obtain discriminant directions in the high-dimensional setting where the number of observations n is much smaller than the ambient dimension p or when features are highly correlated, and analyze the convergence properties of these

methods. The methods are proposed for multi-class sparse discriminant analysis using the sparse optimal scoring formulation with elastic net penalty proposed in [8]; adding both the ℓ_1 - and ℓ_2 -norm penalties gives sparse solutions which, in particular, are competitive when high correlations exist in feature space due to the grouping behaviour of the ℓ_2 -norm. The first two strategies are proximal gradient methods based on modification of the (fast) iterative shrinkage algorithm [4] for linear inverse problems. The third method uses a variant of the alternating direction method of multipliers similar to that proposed in [2]. We will see that these heuristics allow efficient classification of high-dimensional data, which was previously impractical using the current state of the art for sparse discriminant analysis. For example, if a diagonal or low-rank Tikhonov regularization term is used and the number of observations is very small relative to p , then the per-iteration cost of each of our algorithms is $\mathcal{O}(p)$; that is, the per-iteration cost of our approach scales linearly with the number of features of our data. Finally, we provide implementations of our algorithms in the form of the R package **accSDA**(see [12]) and **Matlab** software ¹.

1.1 Contributions

The proposed optimization algorithms are not inherently novel, as they are specializations of existing algorithmic frameworks widely used in sparse regression. However, the application of these proximal algorithms to solve the sparse optimal scoring problem is novel. Moreover, this specialization highlights the strong relationship between the optimal scoring and regression: optimal scoring generalizes regression, in the sense that optimal scoring simultaneously fits both a linear model and a quantitative encoding of categorical class labels.

Further, the proposed sparse optimal scoring heuristics offer a substantial improvement upon the current state of the art for optimal scoring, in terms of both classification accuracy and computational efficiency. Specifically, we show that the computation required for each iteration of the proposed algorithms scales linearly with the number of predictor variables, which yields a significant improvement upon the cubic scaling of the least angle regression-based algorithm initially adopted in [8]; our comparison of computational complexity can be found in Section 2.4 and Appendix A. Moreover, we performed a detailed empirical analysis of our proposed heuristics for sparse optimal scoring, including comparisons of classification accuracy and computational complexity for simulated data and real-world data sets drawn from the UC Riverside Time Series Archive [9,10], investigation of convergence phenomena, and scaling tests. These empirical results agree with our theoretical analyses of computational complexity (Sect. 2.4, App. A) and convergence (Sect. 2.5).

1.2 Existing approaches for sparse LDA

We begin with a brief overview of existing sparse discriminant analysis techniques. Methods such as [14,41,43] assume independence between the features in the given data. This can lead to poor performance in terms of feature selection as well as predictions, in particular when high correlations exist. Thresholding methods such as [39], although proven to be asymptotically optimal, ignore the existing multi-linear correlations when thresholding low correlation estimates. Thresholding, furthermore, does not guarantee an invertible correlation matrix, and often pseudo-inverses must be utilized.

For two-class problems, the analysis of [27] established an equivalence between the three methods described in [8,26,44]. These three approaches are formulated as constrained versions of Fisher’s discriminant problem, the optimal scoring problem, and a least squares formulation of linear discriminant analysis, respectively. For scaled regularization parameters, [27] showed that they all behave asymptotically as Bayes rules. Another two-class sparse linear discriminant method is the linear programming discriminant method proposed in [7], which finds an ℓ_1 -norm penalized estimate of the product between covariance matrix and difference in means.

The sparse optimal scoring (SOS) problem was originally formulated in [8] as a multi-class problem seeking at most $K - 1$ sparse discriminating directions, where K is the number of classes present, whereas [27] was formulated for binary problems. This approach builds on earlier work by Hastie et. al [20,21]. Mai and Zou later proposed a multi-class sparse discriminant analysis (MSDA) based on the Bayes rule formulation of linear discriminant analysis in [28]. It imposes only the ℓ_1 -norm penalty, whereas the SOS imposes an elastic net penalty (ℓ_1 - plus ℓ_2 -norm). Adding the ℓ_2 -norm can give better predictive performance, in particular

¹Available at <http://bpames.people.ua.edu/software>

when very high correlations exist in data. MSDA, furthermore, finds all discriminative directions at once, whereas SOS finds them sequentially via deflation. A sequential solution can be an advantage if the number of classes is high, and a solution involving only a few directions (the most discriminating ones) is needed. On the other hand, if K is small, finding all directions at once may be advantageous, in order to not propagate errors in a sequential manner. Sparse optimal scoring models based on the group-LASSO are considered in [30, 38], while sparse optimal scoring and sparse discriminant analysis has become a popular tool in cognitive neuroscience [19], among many other domains.

Finally, the zero-variance sparse discriminant analysis approach of [2] reformulates the sparse discriminant analysis problem as an ℓ_1 -penalized nonconvex optimization problem in order to sequentially identify discriminative directions in the null-space of the pooled within-class scatter matrix. Most relevant for our discussion here is the use of proximal methods to approximately solve the nonconvex optimization problems in [2]; we will adopt a similar approach for solving the SOS problem.

1.3 Notation

Before we proceed, we first summarize the notation that is used throughout the text. We denote the space of p -dimensional vectors by \mathbf{R}^p and the space of m by n real matrices by $\mathbf{R}^{m \times n}$. Bold capital letters, e.g., \mathbf{X} , will be used to denote matrices, lower-case bold letters, e.g., \mathbf{x} , $\boldsymbol{\beta}$, denote vectors, and unbolded letters will denote scalars (unless otherwise noted). We denote the p -dimensional all-zeros and all-ones vectors by $\mathbf{0}_p$ and \mathbf{e}_p ; we omit the subscript p when the dimension is clear by context. We denote the transpose of a matrix \mathbf{X} by \mathbf{X}^T and the inverse of (nonsingular) \mathbf{X} by \mathbf{X}^{-1} . On the other hand, we use lower-case superscripts to indicate the indices of elements of sequences of vectors, e.g., $\{\mathbf{x}^i\}_{i=0}^\infty = \mathbf{x}^0, \mathbf{x}^1, \dots$ and use subscripts to denote the indices of elements of sequences of scalars, e.g., $\{\alpha_i\}_{i=0}^\infty = \alpha_0, \alpha_1, \dots$. Subscripts will also indicate indices of entries of vectors and matrices; for example, the value in the first row and second column of matrix \mathbf{X} will be denoted by x_{12} . We will reserve the character L to denote the Lipschitz constant of a given Lipschitz continuous operator $g : \mathbf{R}^p \mapsto \mathbf{R}^m$. Conversely, we will use the notation \mathcal{L}_μ to denote the augmented Lagrangian with respect to parameter μ of a given equally constrained optimization problem; we will also use \mathcal{L} to denote the (unaugmented) Lagrangian function. Finally, we denote the *subdifferential*, i.e., the set of subgradients, of a function $f : \mathbf{R}^n \mapsto \mathbf{R}$ at vector \mathbf{x} by

$$\partial f(\mathbf{x}) = \left\{ \phi \in \mathbf{R}^n : f(\mathbf{y}) \geq f(\mathbf{x}) + \phi^T(\mathbf{y} - \mathbf{x}) \text{ for all } \mathbf{y} \in \text{dom} f \right\}.$$

2 Proximal Methods for Sparse Discriminant Analysis

In this section, we describe a block coordinate descent approach for approximately solving the sparse optimal scoring problem for linear discriminant analysis. Proposed in [21], the optimal scoring problem recasts linear discriminant analysis as a generalization of linear regression where both the response variable, corresponding to an optimal labeling or scoring of the classes, and linear model parameters, which yield the discriminant vector, are sought. Specifically, suppose that we have the $n \times p$ data matrix \mathbf{X} , where the rows of \mathbf{X} correspond to observations in \mathbf{R}^p sampled from one of K classes; we assume that the data has been centered so that the sample mean is the zero vector $\mathbf{0} \in \mathbf{R}^p$. Optimal scoring generates a sequence of discriminant vectors and conjugate scoring vectors as follows. Suppose that we have identified the first $j-1$ discriminant vectors $\boldsymbol{\beta}_1, \dots, \boldsymbol{\beta}_{j-1} \in \mathbf{R}^p$ and scoring vectors $\boldsymbol{\theta}_1, \dots, \boldsymbol{\theta}_{j-1} \in \mathbf{R}^K$. To calculate the j th discriminant vector $\boldsymbol{\beta}_j$ and scoring vector $\boldsymbol{\theta}_j$, we solve the optimal scoring criterion problem

$$\begin{aligned} \arg \min_{\boldsymbol{\theta} \in \mathbf{R}^K, \boldsymbol{\beta} \in \mathbf{R}^p} \quad & \|\mathbf{Y}\boldsymbol{\theta} - \mathbf{X}\boldsymbol{\beta}\|^2 \\ \text{s.t.} \quad & \frac{1}{n}\boldsymbol{\theta}^T \mathbf{Y}^T \mathbf{Y} \boldsymbol{\theta} = 1, \quad \boldsymbol{\theta}^T \mathbf{Y}^T \mathbf{Y} \boldsymbol{\theta}_\ell = 0 \quad \forall \ell < j, \end{aligned} \tag{1}$$

where \mathbf{Y} denotes the $n \times K$ indicator matrix for class membership, defined by $y_{\ell m} = 1$ if the ℓ th observation belongs to the m th class, and $y_{\ell m} = 0$ otherwise, and $\|\cdot\| : \mathbf{R}^n \rightarrow \mathbf{R}$ denotes the vector ℓ_2 -norm on \mathbf{R}^n defined by $\|\mathbf{y}\| = \sqrt{y_1^2 + y_2^2 + \dots + y_n^2}$ for all $\mathbf{y} \in \mathbf{R}^n$. We direct the reader to [21] for further details regarding the derivation of (1). A variant of the optimal scoring problem which employs regularization via the elastic net penalty function is proposed in [8]. As before, suppose that we have identified the first $j-1$

discriminant vectors $\beta_1, \dots, \beta_{j-1}$ and scoring vectors $\theta_1, \dots, \theta_{j-1}$. We calculate the j th sparse discriminant vector β_j and scoring vector θ_j as the optimal solutions of the optimal scoring criterion problem

$$\begin{aligned} \arg \min_{\theta \in \mathbf{R}^K, \beta \in \mathbf{R}^p} \quad & \|Y\theta - X\beta\|^2 + \gamma\beta^T \Omega \beta + \lambda\|\beta\|_1 \\ \text{s.t.} \quad & \frac{1}{n}\theta^T Y^T Y \theta = 1, \quad \theta^T Y^T Y \theta_\ell = 0 \quad \forall \ell < j, \end{aligned} \quad (2)$$

where $\|\cdot\|_1 : \mathbf{R}^p \rightarrow \mathbf{R}$ denotes the vector ℓ_1 -norm on \mathbf{R}^p defined by $\|x\|_1 = |x_1| + |x_2| + \dots + |x_p|$ for all $x \in \mathbf{R}^p$, $Y \in \mathbf{R}^{n \times K}$ is again the indicator matrix for class membership, λ and γ are nonnegative tuning parameters, and Ω is a $p \times p$ positive definite matrix. That is, (2) is the result of adding regularization to the optimal scoring problem using a linear combination of the Tikhonov penalty term $\beta^T \Omega \beta$ and the ℓ_1 -norm penalty $\|\beta\|_1$; we will provide further discussion regarding the choice of Ω in Section 2.4. The optimization problem (2) is nonconvex, due to the presence of nonconvex spherical constraints. As such, we do not expect to find a globally optimal solution of (2) using iterative methods. Clemmensen et al. propose a block coordinate descent method to solve (2) in [8]. Suppose that we have an estimate (θ^i, β^i) of (θ_j, β_j) after i iterations. To update θ^i , we fix $\beta = \beta^i$ and solve the optimization problem

$$\begin{aligned} \theta^{i+1} = \arg \min_{\theta \in \mathbf{R}^K} \quad & \|Y\theta - X\beta^i\|^2 \\ \text{s.t.} \quad & \frac{1}{n}\theta^T Y^T Y \theta = 1, \quad \theta^T Y^T Y \theta_\ell = 0 \quad \forall \ell < j. \end{aligned} \quad (3)$$

The subproblem (3) is nonconvex in θ , however, it is known that (3) admits an analytic solution and can be solved exactly in polynomial time. Indeed, we have the following lemma providing an analytic update formula for θ . Note that this update requires $\mathcal{O}(K^3 + pn)$ floating point operations to perform the necessary matrix products. See [8, Section 2.2] for more details.

Lemma 2.1 *The problem (3) has optimal solution*

$$\theta^{i+1} = s \left(I - \frac{1}{n} Q_j Q_j^T Y^T Y \right) (Y^T Y)^{-1} Y^T X \beta^i, \quad (4)$$

where Q_j is the $K \times j$ matrix with columns consisting of the $j-1$ scoring vectors $\theta_1, \dots, \theta_{j-1}$ and the all-ones vector $\mathbf{e} \in \mathbf{R}^K$, and s is a proportionality constant ensuring that $(\theta^{i+1})^T Y^T Y \theta^{i+1} = n$. In particular, θ^{i+1} is given by

$$w = \left(I - \frac{1}{n} Q_j Q_j^T Y^T Y \right) (Y^T Y)^{-1} Y^T X \beta^i, \quad \theta^{i+1} = \frac{\sqrt{n}w}{\|Yw\|}. \quad (5)$$

Proof: We note that (3) has trivial solution $\theta = \mathbf{e}$ for every $\beta = \beta^i \in \mathbf{R}^p$ and $j = 1$. Indeed, $Y\mathbf{e} = \mathbf{e}$ by the structure of the indicator matrix Y and $\sum_{i=1}^n x_{ij} = 0$ for all $j = 1, 2, \dots, p$ because our data has been centered to have sample mean equal to $\mathbf{0}$. Therefore, we may reformulate (3) as

$$\begin{aligned} \min_{\theta \in \mathbf{R}^K} \quad & \|Y\theta - X\beta\|^2 \\ \text{s.t.} \quad & \theta^T Y^T Y \theta = n, \\ & \theta^T Y^T Y \mathbf{e} = 0, \\ & \theta^T Y^T Y \theta_\ell = 0 \quad \ell < j, \end{aligned} \quad (6)$$

to avoid this trivial solution. We wish to show that (6) has optimal solution $\hat{\theta}$ given by

$$\hat{\theta} = \frac{\sqrt{n}w}{\sqrt{w^T Y^T Y w}}, \quad (7)$$

where $w = (I - \frac{1}{n} Q_j Q_j^T Y^T Y)(Y^T Y)^{-1} Y^T X \beta$.

To do so, note that (6) satisfies the linear independence constraint qualification because the set of constraint function gradients

$$\{2Y^T Y \theta, Y^T Y \mathbf{e}, Y^T Y \theta_1, \dots, Y^T Y \theta_{j-1}\}$$

is linearly independent. Moreover, the optimal value of (6) is bounded below by 0. Therefore, (6) has global minimizer, $\hat{\boldsymbol{\theta}}$, which must satisfy the Karush-Kuhn-Tucker conditions, i.e., there exists $\mathbf{v} \in \mathbf{R}^k$, $\psi \in \mathbf{R}$ such that

$$\mathbf{Y}^T \mathbf{Y} \hat{\boldsymbol{\theta}} - \mathbf{Y}^T \mathbf{X} \boldsymbol{\beta} + \psi \mathbf{Y}^T \mathbf{Y} \hat{\boldsymbol{\theta}} + \mathbf{Y}^T \mathbf{Y} \mathbf{Q}_j \mathbf{v} = \mathbf{0}, \quad (8)$$

where $\mathbf{Q}_j = [\mathbf{e}, \boldsymbol{\theta}_1, \boldsymbol{\theta}_2, \dots, \boldsymbol{\theta}_{j-1}]$. We consider the following two cases.

First, suppose that $\mathbf{Y}^T \mathbf{X} \boldsymbol{\beta} \notin \text{range}(\mathbf{Y}^T \mathbf{Y} \mathbf{Q}_j)$. Rearranging (8) yields

$$\hat{\boldsymbol{\theta}} = \frac{1}{1 + \psi} (\mathbf{Y}^T \mathbf{Y})^{-1} (\mathbf{Y}^T \mathbf{X} \boldsymbol{\beta} - \mathbf{Y}^T \mathbf{Y} \mathbf{Q}_j \mathbf{v}). \quad (9)$$

We choose the dual variables ψ and \mathbf{v} so that $\hat{\boldsymbol{\theta}}$ is feasible for (6). It is easy to see that the conjugacy constraints are equivalent to $\mathbf{Q}_j^T \mathbf{Y}^T \mathbf{Y} \hat{\boldsymbol{\theta}} = \mathbf{0}$, which holds if and only if

$$\begin{aligned} \mathbf{0} &= \mathbf{Q}_j^T (\mathbf{Y}^T \mathbf{X} \boldsymbol{\beta} - \mathbf{Y}^T \mathbf{Y} \mathbf{Q}_j \mathbf{v}) = \mathbf{Q}_j^T \mathbf{Y}^T \mathbf{X} \boldsymbol{\beta} - \mathbf{Q}_j^T \mathbf{Y}^T \mathbf{Y} \mathbf{Q}_j \mathbf{v} \\ &= \mathbf{Q}_j^T \mathbf{Y}^T \mathbf{X} \boldsymbol{\beta} - n \mathbf{v}, \end{aligned}$$

where the last equality follows from the fact that $\mathbf{e}^T \mathbf{Y}^T \mathbf{Y} \mathbf{e} = \boldsymbol{\theta}_i^T \mathbf{Y}^T \mathbf{Y} \boldsymbol{\theta}_i = n$ for all $i = 1, 2, \dots, j-1$. It follows immediately that

$$\mathbf{v} = \frac{1}{n} \mathbf{Q}_j^T \mathbf{Y}^T \mathbf{X} \boldsymbol{\beta}. \quad (10)$$

Substituting (10) into (9) yields

$$\begin{aligned} \hat{\boldsymbol{\theta}} &= \frac{1}{1 + \psi} \left((\mathbf{Y}^T \mathbf{Y})^{-1} \mathbf{Y}^T \mathbf{X} \boldsymbol{\beta} - \frac{1}{n} \mathbf{Q}_j \mathbf{Q}_j^T \mathbf{Y}^T \mathbf{X} \boldsymbol{\beta} \right) \\ &= \frac{1}{1 + \psi} \left(\mathbf{I} - \frac{1}{n} \mathbf{Q}_j \mathbf{Q}_j^T \mathbf{Y}^T \mathbf{Y} \right) (\mathbf{Y}^T \mathbf{Y})^{-1} \mathbf{Y}^T \mathbf{X} \boldsymbol{\beta} \\ &= \frac{1}{1 + \psi} \mathbf{w}, \end{aligned} \quad (11)$$

where we choose $\psi \in \mathbf{R}$ so that $\hat{\boldsymbol{\theta}}^T \mathbf{Y}^T \mathbf{Y} \hat{\boldsymbol{\theta}} = n$:

$$\sqrt{n}(1 + \psi) = \pm \sqrt{\mathbf{w}^T \mathbf{Y}^T \mathbf{Y} \mathbf{w}} = \pm \|\mathbf{Y} \mathbf{w}\|. \quad (12)$$

To complete the argument, note that

$$\begin{aligned} \|\mathbf{Y} \hat{\boldsymbol{\theta}} - \mathbf{X} \boldsymbol{\beta}\|^2 &= n \mp \frac{2\sqrt{n}}{\|\mathbf{Y} \mathbf{w}\|} \boldsymbol{\beta}^T \mathbf{X}^T \left(\mathbf{I} - \frac{1}{n} \mathbf{Q}_j \mathbf{Q}_j^T \mathbf{Y}^T \mathbf{Y} \right) (\mathbf{Y}^T \mathbf{Y})^{-1} \mathbf{Y}^T \mathbf{X} \boldsymbol{\beta} \\ &\quad + \|\mathbf{X} \boldsymbol{\beta}\|^2. \end{aligned}$$

Note further that the matrix $\mathbf{Y} \mathbf{Q}_j \mathbf{Q}_j^T \mathbf{Y}^T$ has decomposition

$$\mathbf{Y} \mathbf{Q}_j \mathbf{Q}_j^T \mathbf{Y}^T = \mathbf{Y} \mathbf{e} \mathbf{e}^T \mathbf{Y}^T + \mathbf{Y} \boldsymbol{\theta}_1 \boldsymbol{\theta}_1^T \mathbf{Y}^T + \dots + \mathbf{Y} \boldsymbol{\theta}_{j-1} \boldsymbol{\theta}_{j-1}^T \mathbf{Y}^T.$$

The conjugacy of the columns of \mathbf{Q}_j implies that eigenvectors of $\mathbf{Y} \mathbf{Q}_j \mathbf{Q}_j^T \mathbf{Y}^T$ are $\mathbf{Y} \boldsymbol{\theta}_1, \dots, \mathbf{Y} \boldsymbol{\theta}_{j-1}$, and $\mathbf{Y} \mathbf{e}$, each with eigenvalue n ; since $\mathbf{Y} \mathbf{Q}_j \mathbf{Q}_j^T \mathbf{Y}^T$ has rank equal to k , all remaining eigenvalues of $\mathbf{Y} \mathbf{Q}_j \mathbf{Q}_j^T \mathbf{Y}^T$ must be equal to 0. Moreover, for any $\mathbf{z} = \mathbf{Y} \boldsymbol{\theta}_i$, $i = 1, 2, \dots, j-1$, or $\mathbf{z} = \mathbf{Y} \mathbf{e}$, we have

$$\mathbf{Y} \left((\mathbf{Y}^T \mathbf{Y})^{-1} - \frac{1}{n} \mathbf{Q}_j \mathbf{Q}_j^T \right) \mathbf{Y}^T \mathbf{z} = \mathbf{z} - \mathbf{z} = \mathbf{0}.$$

The matrix $(\mathbf{Y}^T \mathbf{Y})^{-1}$ is a positive definite diagonal matrix, with i th diagonal entry $1/|C_i|$, where $|C_i|$ denotes the number of observations belonging to class i ; this implies that $\mathbf{Y}(\mathbf{Y}^T \mathbf{Y})^{-1} \mathbf{Y}^T$ is positive semidefinite.

This establishes that the matrix $\mathbf{Y}((\mathbf{Y}^T \mathbf{Y})^{-1} - \frac{1}{n} \mathbf{Q}_j \mathbf{Q}_j^T) \mathbf{Y}^T$ is positive semidefinite and, thus, $\|\mathbf{Y}\boldsymbol{\theta} - \mathbf{X}\boldsymbol{\beta}\|^2$ is minimized by $\hat{\boldsymbol{\theta}}$ with $\psi = +\|\mathbf{Y}\mathbf{w}\|/\sqrt{n} - 1$.

Second, suppose that $\mathbf{Y}^T \mathbf{X}\boldsymbol{\beta} \in \text{range}(\mathbf{Y}^T \mathbf{Y} \mathbf{Q}_j)$. This implies that there exists some $\mathbf{v} \in \mathbf{R}^K$ such that

$$\mathbf{Y}^T \mathbf{X}\boldsymbol{\beta} = \mathbf{Y}^T \mathbf{Y} \mathbf{Q}_j \mathbf{v}.$$

Substituting into the objective of (6), we see that

$$\begin{aligned} \|\mathbf{Y}\boldsymbol{\theta} - \mathbf{X}\boldsymbol{\beta}\|^2 &= \boldsymbol{\theta}^T \mathbf{Y}^T \mathbf{Y} \boldsymbol{\theta} - 2\boldsymbol{\theta}^T \mathbf{Y}^T \mathbf{X}\boldsymbol{\beta} + \boldsymbol{\beta}^T \mathbf{X}^T \mathbf{X} \boldsymbol{\beta} \\ &= n - 2\boldsymbol{\theta}^T \mathbf{Y}^T \mathbf{Y} \mathbf{Q}_j \mathbf{v} + \boldsymbol{\beta}^T \mathbf{X}^T \mathbf{X} \boldsymbol{\beta} \\ &= n + \boldsymbol{\beta}^T \mathbf{X}^T \mathbf{X} \boldsymbol{\beta} \end{aligned}$$

for every feasible solution $\boldsymbol{\theta}$ of (6). This implies that every feasible solution of (6) is also optimal in this case. In particular, $\hat{\boldsymbol{\theta}}$ given by (11) is feasible for (6) and, therefore, optimal. ■

After we have updated $\boldsymbol{\theta}^{i+1}$, we obtain $\boldsymbol{\beta}^{i+1}$ by solving the unconstrained optimization problem

$$\boldsymbol{\beta}^{i+1} = \arg \min_{\boldsymbol{\beta} \in \mathbf{R}^p} \|\mathbf{Y}\boldsymbol{\theta}^{i+1} - \mathbf{X}\boldsymbol{\beta}\|^2 + \gamma \boldsymbol{\beta}^T \boldsymbol{\Omega} \boldsymbol{\beta} + \lambda \|\boldsymbol{\beta}\|_1. \quad (13)$$

That is, we update $\boldsymbol{\beta}^{i+1}$ by solving the generalized elastic net problem (13). We stop this block update scheme if the relative change in consecutive iterates is smaller than a desired tolerance. Specifically, we stop the algorithm if

$$\max \left\{ \frac{\|\boldsymbol{\theta}^{i+1} - \boldsymbol{\theta}^i\|}{\|\boldsymbol{\theta}^{i+1}\|}, \frac{\|\boldsymbol{\beta}^{i+1} - \boldsymbol{\beta}^i\|}{\|\boldsymbol{\beta}^{i+1}\|} \right\} \leq \epsilon$$

for stopping tolerance $\epsilon > 0$.

It is suggested in [8] that (2) can be solved using the *least angle regression (LARS)* algorithm proposed in [45]. Unfortunately, this approach carries a computational cost on the order of $\mathcal{O}(mnp + m^3)$, where m is the desired number of nonzero coefficients, which is prohibitively expensive if both p and m are large. For example, if $m = cp$ for some constant $c \in (0, 1)$, then the per-iteration cost scales cubically with p . We should also note that coordinate descent methods have been widely adopted for calculation of elastic net regularized generalized linear models; see [16] for further details. However, we are unaware of any application of coordinate descent methods for solution of the elastic net regularized optimal scoring problem (2).

Our primary contribution is a collection of algorithms for solving the elastic net problem (13). Specifically, we specialize three classical algorithms, each based on the evaluation of proximal operators, to obtain novel numerical methods for solution of the sparse optimal scoring problem. We will see that these algorithms require significantly fewer computational resources than least angle regression if we exploit structure in the regularization parameter $\boldsymbol{\Omega}$.

2.1 Proximal Algorithms for the Generalized Elastic Net Problem

Given a convex function $f : \mathbf{R}^p \rightarrow \mathbf{R}$, the *proximal operator* $\text{prox}_f : \mathbf{R}^p \rightarrow \mathbf{R}^p$ of f is defined by

$$\text{prox}_f(\mathbf{y}) = \arg \min_{\mathbf{x} \in \mathbf{R}^p} \left\{ f(\mathbf{x}) + \frac{1}{2} \|\mathbf{x} - \mathbf{y}\|^2 \right\},$$

which yields a point that balances the competing objectives of being near \mathbf{y} while simultaneously minimizing f . The use of proximal operators is a classical technique in optimization, particularly as surrogates for gradient descent steps for minimization of nonsmooth functions. For example, consider the optimization problem

$$\min_{\mathbf{x} \in \mathbf{R}^p} f(\mathbf{x}) + g(\mathbf{x}), \quad (14)$$

where $f : \mathbf{R}^p \rightarrow \mathbf{R}$ is differentiable and $g : \mathbf{R}^p \rightarrow \mathbf{R}$ is potentially nonsmooth. That is, (14) minimizes an objective that can be decomposed as the sum of a differentiable function f and nonsmooth function g . To solve (14), the *proximal gradient method* performs iterations consisting of a step in the direction of the

Algorithm 1: Block Coordinate Descent for SDA (2)

Data: Given stopping tolerance ϵ , and maximum number of iterations N .

Result: Discriminant vectors $(\theta_1^*, \beta_1^*), (\theta_2^*, \beta_2^*), \dots, (\theta_{K-1}^*, \beta_{K-1}^*)$ calculated as approximate solutions of (2).

for $j = 1, 2, \dots, K - 1$

 Initialize θ_j^0 as the projection of K -dimensional vector \mathbf{z} with entries sampled uniformly at random from the interval $[0, 1]$ onto the feasible region using the identity

$$\theta_j^0 = \left(I - \frac{1}{n} \mathbf{Q}_j \mathbf{Q}_j^T \mathbf{Y}^T \mathbf{Y} \right) (\mathbf{Y}^T \mathbf{Y})^{-1} \mathbf{z}, \quad \theta_j^0 = \frac{\sqrt{n} \theta_j^0}{\|\mathbf{Y} \theta_j^0\|};$$

 Calculate the j th scoring and discriminant vector pair (θ_j^*, β_j^*) as the limit point of the sequence $\{(\theta_j^i, \beta_j^i)\}_{i=0}^\infty$ as follows:

for $i = 0, 1, 2 \dots N$

 Update β_j^i as the solution of (13) with $\theta = \theta_j^i$ using the solution returned by one of (3), (4), (6), and (5);

 Update θ_j^{i+1} by

$$\mathbf{w} = \left(I - \frac{1}{n} \mathbf{Q}_j \mathbf{Q}_j^T \mathbf{Y}^T \mathbf{Y} \right) (\mathbf{Y}^T \mathbf{Y})^{-1} \mathbf{Y}^T \mathbf{X} \beta_j^i, \quad \theta_j^{i+1} = \frac{\sqrt{n} \mathbf{w}}{\|\mathbf{Y} \mathbf{w}\|};$$

 Declare convergence if the residual between consecutive iterates is smaller than desired tolerance:

if $\max \left\{ \frac{\|\theta_j^{i+1} - \theta_j^i\|}{\|\theta_j^{i+1}\|}, \frac{\|\beta_j^{i+1} - \beta_j^i\|}{\|\beta_j^{i+1}\|} \right\} < \epsilon$

 The algorithm has converged;

break;

end

end

end

negative gradient $-\nabla f$ of the smooth part f followed by evaluation of the proximal operator of g : given iterate \mathbf{x}^i , we obtain the updated iterate \mathbf{x}^{i+1} by

$$\mathbf{x}^{i+1} = \underset{\alpha_i g}{\text{prox}}(\mathbf{x}^i - \alpha_i \nabla f(\mathbf{x}^i)), \quad (15)$$

where α_i is a step length parameter. If both f and g are differentiable and the step size α_i is small, then this approach reduces to the classical gradient descent iteration: $\mathbf{x}^{i+1} \approx \mathbf{x}^i - \alpha_i \nabla f(\mathbf{x}^i) - \alpha_i \nabla g(\mathbf{x}^i)$. We direct the reader to the recent survey article [37] for more details regarding the proximal gradient method and proximal operators in general.

In [4], Beck and Teboulle consider a specialization of the proximal gradient method, called the *iterative soft-thresholding algorithm (ISTA)*, to the ℓ_1 -regularized linear inverse problem

$$\min_{\mathbf{x} \in \mathbf{R}^n} \|\mathbf{A} \mathbf{x} - \mathbf{b}\|^2 + \lambda \|\mathbf{x}\|_1, \quad (16)$$

where $\mathbf{A} \in \mathbf{R}^{m \times n}$, $\mathbf{b} \in \mathbf{R}^m$ are known, and $\lambda > 0$ is a regularization parameter chosen by the user; \mathbf{b} is often a vector of noisy measurements of an unknown vector or signal \mathbf{x} by the sampling matrix \mathbf{A} . The primary contribution of [4] is an accelerated variant of ISTA, called *fast iterative soft-threshold (FISTA)*, and a convergence analysis establishing the non-asymptotic global rate of convergence of both ISTA and FISTA; we'll delay further discussion of FISTA until Section 2.2. Although motivated by the linear inverse problem (16), the analysis of [4] focuses on the more general problem of minimizing the sum $f + g$, where f is differentiable with Lipschitz continuous gradient and g is potentially nonsmooth. In this case, a Lipschitz

Algorithm 2: Backtracking algorithm for ISTA

Data: Given $L_0 > 0$, scaling parameter $\eta > 1$, stopping tolerance ϵ , and maximum number of iterations N .

Result: Minimizer \mathbf{x}^* of F .

for $i = 0, 1, 2, \dots, N$

 Update iterate \mathbf{x}^{i+1} using proximal gradient step and backtracking line search:

while *step size is not accepted*

 Update step length

$$\bar{L} = \eta^k L_{i-1}, \quad \alpha = \frac{1}{\bar{L}};$$

 Update iterate using proximal gradient step (15):

$$\mathbf{x}^{i+1} = \underset{\bar{\alpha}g}{\text{prox}} \left(\mathbf{x}^i + \bar{\alpha} \nabla f(\mathbf{x}^i) \right).$$

 Determine whether to accept update or increment step length:

if $F(\mathbf{x}^{i+1}) \leq f(\mathbf{x}^i) + \nabla f(\mathbf{x}^i)^T(\mathbf{x}^{i+1} - \mathbf{x}^i) + \frac{\bar{L}}{2} \|\mathbf{x}^{i+1} - \mathbf{x}^i\|^2 + g(\mathbf{x}^{i+1})$

 Accept update: $L_i = \bar{L}$, $\alpha_i = \bar{\alpha}$. ;

break;

else

 Do not accept update: $k \leftarrow k + 1$;

end

end

 Declare convergence if $\mathbf{0}$ is in the subdifferential of the objective function:

if *there exists $\phi \in \partial g(\mathbf{x}^{i+1})$ such that $\|\nabla f(\mathbf{x}^{i+1}) + \phi\|_\infty < \epsilon$*

 The algorithm has converged;

break;

end

end

constant of ∇f is used as a constant step size in (15) or the step length is chosen using a backtracking line search as in Algorithm 2. The following theorem establishes that the sequence of iterates generated converges sublinearly to the optimal function value of $F := f + g$ at a rate no worse than $\mathcal{O}(1/i)$, where i indicates the number of iterations performed so far; see [4, Theorem 3.1].

Theorem 2.1 *Let the function $F : \mathbf{R}^n \rightarrow \mathbf{R}$ be decomposable as $F(\mathbf{x}) = f(\mathbf{x}) + g(\mathbf{x})$, where f is differentiable with Lipschitz continuous gradient; let L be a Lipschitz constant such that $\|\nabla f(\mathbf{x}) - \nabla f(\mathbf{y})\| \leq L\|\mathbf{x} - \mathbf{y}\|$ for all $\mathbf{x}, \mathbf{y} \in \mathbf{R}^n$. Suppose that F has unique minimizer $\mathbf{x}^* \in \mathbf{R}^n$. Let $\{\mathbf{x}^i\}_{i=0}^\infty$ be the sequence of iterates generated by (15) with constant step size $\alpha = 1/L$ or by Algorithm 2. Then there exists a constant $c > 0$ such that*

$$F(\mathbf{x}^i) - F(\mathbf{x}^*) \leq \frac{cL\|\mathbf{x}^0 - \mathbf{x}^*\|^2}{i} \quad (17)$$

for all i .

Expanding the residual norm term $\|\mathbf{Y}\boldsymbol{\theta} - \mathbf{X}\boldsymbol{\beta}\|^2$ in the objective of (13) and dropping the constant term shows that (13) is equivalent to minimizing

$$F(\boldsymbol{\beta}) = \frac{1}{2}\boldsymbol{\beta}^T \mathbf{A}\boldsymbol{\beta} + \mathbf{d}^T \boldsymbol{\beta} + \lambda\|\boldsymbol{\beta}\|_1, \quad (18)$$

where $\mathbf{A} = 2(\mathbf{X}^T \mathbf{X} + \gamma \boldsymbol{\Omega})$ and $\mathbf{d} = -2\mathbf{X}^T \mathbf{Y}\boldsymbol{\theta}^{i+1}$. We can decompose F as $F(\boldsymbol{\beta}) = f(\boldsymbol{\beta}) + g(\boldsymbol{\beta})$, where $f(\boldsymbol{\beta}) = \frac{1}{2}\boldsymbol{\beta}^T \mathbf{A}\boldsymbol{\beta} + \mathbf{d}^T \boldsymbol{\beta}$ and $g(\boldsymbol{\beta}) = \lambda\|\boldsymbol{\beta}\|_1$. Note that F is strongly convex if the penalty matrix $\boldsymbol{\Omega}$ is positive definite; in this case (18) has a unique minimizer. Note further that f is differentiable with $\nabla f(\boldsymbol{\beta}) = \mathbf{A}\boldsymbol{\beta} + \mathbf{d}$.

Algorithm 3: Proximal gradient method for solving the elastic net subproblem (13)

Data: Given initial iterate β^0 , sequence of step sizes $\{\alpha_i\}_{i=0}^\infty$, stopping tolerance ϵ , and maximum number of iterations N .

Result: Solution β^* of (13).

for $i = 0, 1, 2 \dots N$

 Update gradient term by (20):

$$\mathbf{p}^i = \beta^i - \alpha_i(\mathbf{A}\beta^i + \mathbf{d});$$

 Update iterate using proximal gradient step (19):

$$\beta^{i+1} = \text{sign}(\mathbf{p}^i) \max\{|\mathbf{p}^i| - \lambda\alpha_i\mathbf{e}, \mathbf{0}\};$$

 Terminate if current iterate is approximately stationary:

if $\|\mathbf{A}\beta^{i+1} + \mathbf{d} + \lambda \text{sign}(\beta^{i+1})\|_\infty < p\epsilon$:

 The algorithm has converged;

break;

end

end

Moreover, the proximal operator of the ℓ_1 -norm term $g(\beta) = \lambda\|\beta\|_1$ is given by

$$\text{prox}_{\lambda\|\cdot\|_1}(\mathbf{y}) = \text{sign}(\mathbf{y}) \max\{|\mathbf{y}| - \lambda\mathbf{e}, \mathbf{0}\} =: S_\lambda(\mathbf{y});$$

see [37, Section 6.5.2]. The proximal operator $S_\lambda = \text{prox}_{\lambda\|\cdot\|_1}$ is often called the *soft thresholding operator* (with respect to the threshold λ) and $\text{sign} : \mathbf{R}^p \rightarrow \mathbf{R}^p$ and $\max : \mathbf{R}^p \times \mathbf{R}^p \rightarrow \mathbf{R}^p$ are the element-wise sign and maximum mappings defined by

$$[\text{sign}(\mathbf{y})]_i = \text{sign}(y_i) = \begin{cases} +1, & \text{if } y_i > 0 \\ 0, & \text{if } y_i = 0 \\ -1, & \text{if } y_i < 0 \end{cases}$$

and $[\max(\mathbf{x}, \mathbf{y})]_i = \max(x_i, y_i)$. Using this decomposition, we can apply the proximal gradient method to generate a sequence of iterates $\{\beta^i\}$ by

$$\beta^{i+1} = \text{sign}(\mathbf{p}^i) \max\{|\mathbf{p}^i| - \lambda\alpha_i\mathbf{e}, \mathbf{0}\}, \quad (19)$$

where

$$\mathbf{p}^i = \beta^i - \alpha_i \nabla f(\beta^i) = \beta^i - \alpha_i(\mathbf{A}\beta^i + \mathbf{d}); \quad (20)$$

here, \mathbf{e} and $\mathbf{0}$ denote the all-ones and all-zeros vectors in \mathbf{R}^p , respectively. This proximal gradient algorithm with constant step lengths is summarized in Algorithm 3; Algorithm 2 can be modified to obtain a variant of Algorithm 3 that employs a backtracking line search. It is important to note that this update scheme is virtually identical to that of ISTA. Specifically, our problem and update formula differs only from that typically associated with ISTA in the presence of the Tikhonov regression term $\beta^T \Omega \beta$ in our model. As an immediate consequence, we see that the sequence of function values $\{F(\beta^i)\}$ generated by Algorithm 3, with an appropriate choice of step lengths $\{\alpha_i\}$, converges sublinearly to the optimal function value of (18) at a rate no worse than $\mathcal{O}(1/i)$ (compare to Theorem 2.1).

Theorem 2.2 *Let $\{\beta^i\}$ be generated by Algorithm 3 with initial iterate β^0 and constant step size $\alpha_i = \alpha \in (0, 1/\|\mathbf{A}\|)$ or step sizes chosen using the backtracking scheme given by Algorithm 2, where $\|\mathbf{A}\| = \lambda_{\max}(\mathbf{A})$ denotes the largest eigenvalue of the positive semidefinite matrix \mathbf{A} . Suppose that β^* is a minimizer of F . Then there exists a constant c such that*

$$F(\beta^i) - F(\beta^*) \leq \frac{c\|\mathbf{A}\|\|\beta^0 - \beta^*\|^2}{i} \quad (21)$$

for any $i \geq 1$.

It is known that ISTA converges *linearly* when the objective function F is strongly convex (see [3, Chapter 10]). We will see that the strong convexity of the objective of (2) depends on the structure of the regularization term $\mathbf{\Omega}$. When $\mathbf{\Omega}$ is full rank, then F is strongly convex. Therefore, the sequence of iterates generated by Algorithm 3 converges to the unique minimizer of (13) if the penalty parameter $\mathbf{\Omega}$ is chosen to be positive definite. If we choose $\mathbf{\Omega}$ to be positive semidefinite but not full rank, then F may not be strongly convex. In this case, Theorem 2.2 establishes that the sequence of iterates generated by Algorithm 3 converges sublinearly to the minimum value of (13) and any limit point of this sequence is a minimizer of (13). We will see that using such a matrix may have attractive computational advantages despite this loss of uniqueness.

It is reasonably easy to see that the quadratic term of F in (18) is differentiable and has Lipschitz continuous gradient with constant $L = \|\mathbf{A}\|$; this is the significance of the $\|\mathbf{A}\|$ term in (21). In order to ensure convergence in our proximal gradient method, we need to estimate $\|\mathbf{A}\|$ to choose a sufficiently small step size α . Computing this Lipschitz constant may be prohibitively expensive for large p ; one can typically calculate $\|\mathbf{A}\|$ to arbitrary precision using variants of the Power Method (see [18, Sections 7.3.1, 8.2]) at a cost of $\mathcal{O}(p^2 \log p)$ floating point operations. Instead, we could use an upper bound $\tilde{L} \geq L$ to compute our constant step size $\alpha = 1/\tilde{L} \leq 1/L$. For example, when $\mathbf{\Omega}$ is a diagonal matrix, we estimate $\|\mathbf{A}\|$ by

$$\|\mathbf{A}\| = 2\|\gamma\mathbf{\Omega} + \mathbf{X}^T \mathbf{X}\| \leq 2\gamma\|\text{diag}(\mathbf{\Omega})\|_\infty + 2\|\mathbf{X}\|_F^2 \approx \frac{1}{\alpha},$$

where $\text{diag}(\mathbf{M}) \in \mathbf{R}^p$ is the vector of diagonal entries of the matrix $\mathbf{M} \in \mathbf{R}^{p \times p}$. Here, we used the triangle inequality and the identity $\|\mathbf{X}^T \mathbf{X}\| \leq \|\mathbf{X}\|_F^2$, where $\|\mathbf{X}\|_F$ denotes the Frobenius norm of \mathbf{X} defined by $\|\mathbf{X}\|_F^2 = \sum_{i=1}^n \sum_{j=1}^p x_{ij}^2$. The Frobenius norm and, hence, this estimate of $\|\mathbf{A}\|$ can be computed using only $\mathcal{O}(np)$ floating point operations.

In practice, we stop Algorithm 3 after a maximum number of iterations are performed or a sufficiently suboptimal solution is identified. Recall, that β^* minimizes $F(\beta)$ if $\mathbf{0} \in \partial F(\beta)$. On the other hand, we know that $\mathbf{A}\beta^* + \mathbf{d} + \lambda \text{sign}(\beta^*) \in \partial F(\beta^*)$ by the structure of the subgradients of $\|\beta\|_1$. This implies that we can terminate our proximal gradient update scheme if we find β^* such that $\mathbf{A}\beta^* + \mathbf{d} + \lambda \text{sign}(\beta^*)$ is close to $\mathbf{0}$. Specifically, we stop the iterative scheme after the i th iteration if

$$\|\mathbf{A}\beta^i + \mathbf{d} + \lambda \text{sign}(\beta^i)\|_\infty = \max_j |(\mathbf{A}\beta^i + \mathbf{d} + \lambda \text{sign}(\beta^i))_j| \leq p\epsilon$$

for given stopping tolerance $\epsilon > 0$.

2.2 The Accelerated Proximal Gradient Method

The similarity of our method to iterative soft thresholding and, more generally, our use of proximal gradient steps to mimic the gradient method for minimization of our nonsmooth objective suggests that we may be able to use momentum terms to accelerate convergence of our iterates. In particular, we modify the fast iterative soft thresholding algorithm (FISTA) described in [4, Section 4] to solve our subproblem. This approach extends a variety of accelerated gradient descent methods, most notably those of Nesterov [31–33], to minimization of composite convex functions; for further details regarding the acceleration process and motivation for why such acceleration is possible, we direct the reader to the references [1, 6, 15, 25, 36, 40, 42].

We accelerate convergence of our iterates by taking a proximal gradient step from an extrapolation of the last two iterates. Applied to (14), the accelerated proximal gradient method features updates of the form

$$\mathbf{y}^{i+1} = \mathbf{x}^i + \omega_i(\mathbf{x}^i - \mathbf{x}^{i-1}) \tag{22}$$

$$\mathbf{x}^{i+1} = \text{prox}_{\alpha g}(\mathbf{y}^{i+1} - \alpha \nabla f(\mathbf{y}^{i+1})), \tag{23}$$

where $\omega_i \in [0, 1)$ is an extrapolation parameter; a standard choice of this parameter is $i/(i+3)$. Applying this modification to our original proximal gradient algorithm yields Algorithm 4. Modifying the backtracking line search of Algorithm 2 to use the accelerated proximal gradient update yields Algorithm 5. It can be shown that the sequence of iterates generated by either of these algorithms converges in value to the optimal solution of (13) at rate $\mathcal{O}(1/i^2)$ (see [4, Theorem 4.4]).

Algorithm 4: Accelerated proximal gradient method for solving (13) with constant step size

Data: Given initial iterates $\beta^0 = \beta^1$, step length α , sequence of extrapolation parameters $\{\omega_i\}_{i=0}^\infty$, stopping tolerance ϵ , and maximum number of iterations N .

Result: Solution β^* of (13).

for $i = 1, 2, \dots, N$

 Update momentum term by (22):

$$\mathbf{y}^{i+1} = \beta^i + \omega_i(\beta^i - \beta^{i-1});$$

 Update gradient term by (20):

$$\mathbf{p}^{i+1} = \mathbf{y}^{i+1} - \alpha(\mathbf{A}\mathbf{y}^{i+1} + \mathbf{d});$$

 Update iterate using proximal gradient step (19):

$$\beta^{i+1} = \text{sign}(\mathbf{p}^{i+1}) \max\{|\mathbf{p}^{i+1}| - \lambda\alpha\mathbf{e}, \mathbf{0}\};$$

 Terminate if current iterate is approximately stationary:

if $\|\mathbf{A}\beta^{i+1} + \mathbf{d} + \lambda \text{sign}(\beta^{i+1})\|_\infty < p\epsilon$:

 The algorithm has converged;

break;

end

end

Theorem 2.3 Let $\{\beta^i\}$ be generated by Algorithm 4 and constant step size $\alpha_i = \alpha \in (0, 1/\|\mathbf{A}\|)$ or generated using backtracking line search by Algorithm 5 with initial iterate β^0 . Then there exists constant $c > 0$ such that

$$F(\beta^i) - F(\beta^*) \leq \frac{c\|\mathbf{A}\|\|\beta^0 - \beta^*\|^2}{i^2} \quad (24)$$

for any $i \geq 1$ and minimizer β^* of F .

2.3 The Alternating Direction Method of Multipliers

We conclude by proposing a third algorithm for minimization of (18) based on the *alternating direction method of multipliers* (ADMM) for minimizing separable functions under linear coupling constraints. The ADMM solves problems of the form

$$\min_{\mathbf{x} \in \mathbf{R}^p, \mathbf{y} \in \mathbf{R}^m} \left\{ f(\mathbf{x}) + g(\mathbf{y}) : \mathbf{A}\mathbf{x} + \mathbf{B}\mathbf{y} = \mathbf{c} \right\}, \quad (25)$$

via an approximate dual gradient ascent, where $f : \mathbf{R}^p \rightarrow \mathbf{R}$, $g : \mathbf{R}^m \rightarrow \mathbf{R}$, $\mathbf{A} \in \mathbf{R}^{r \times p}$, $\mathbf{B} \in \mathbf{R}^{r \times m}$, and $\mathbf{c} \in \mathbf{R}^r$; we direct the reader to the recent survey [5] for more details regarding the ADMM.

The minimization of the composite function F defined in (18) can be written as the unconstrained optimization problem

$$\min_{\beta \in \mathbf{R}^p} F(\beta) = \min_{\beta \in \mathbf{R}^p} \frac{1}{2} \beta^T \mathbf{A} \beta + \mathbf{d}^T \beta + \lambda \|\beta\|_1. \quad (26)$$

We can rewrite (26) in an equivalent form appropriate for the ADMM by splitting the decision variable $\beta \in \mathbf{R}^p$ as two new variables $\mathbf{x}, \mathbf{y} \in \mathbf{R}^p$ with an accompanying linear coupling constraint $\mathbf{x} = \mathbf{y}$. Following this change of variables, we can express (26) as

$$\begin{aligned} \min_{\mathbf{x}, \mathbf{y} \in \mathbf{R}^p} \quad & \frac{1}{2} \mathbf{x}^T \mathbf{A} \mathbf{x} + \mathbf{d}^T \mathbf{x} + \lambda \|\mathbf{y}\|_1 \\ \text{s.t.} \quad & \mathbf{x} - \mathbf{y} = \mathbf{0}. \end{aligned} \quad (27)$$

Algorithm 5: Accelerated proximal gradient method for solving (13) with backtracking line search

Data: Initial iterates $\beta^0 = \beta^1$, initial Lipschitz constant $L_0 > 0$, scaling parameter $\eta > 1$, sequence of extrapolation parameters $\{\omega_i\}_{i=0}^\infty$, stopping tolerance ϵ , and maximum number of iterations N .

Result: Solution β^* of (13).

for $i = 0, 1, 2 \dots N$

 Update β^{i+1} using accelerated proximal gradient step and backtracking line search:

for $k = 0, 1, 2 \dots$ until step size accepted

 Update step length:

$$\bar{L} = \eta^k L_i, \quad \alpha = \frac{1}{\bar{L}};$$

 Update iterate using accelerated proximal gradient step (19):

$$\begin{aligned} \mathbf{y}^{i+1} &= \beta^i + \omega_i(\beta^i - \beta^{i-1}) \\ \mathbf{p}^{i+1} &= \mathbf{y}^{i+1} - \alpha(\mathbf{A}\mathbf{y}^{i+1} + \mathbf{d}) \\ \beta^{i+1} &= \text{sign}(\mathbf{p}^{i+1}) \max\{|\mathbf{p}^{i+1}| - \lambda\alpha\mathbf{e}, \mathbf{0}\}; \end{aligned}$$

 Determine whether to accept update or increment step length:

$$\text{if } (\beta^{i+1} - \mathbf{y}^{i+1})^T \left(\frac{\bar{L}}{2} \mathbf{I} - \mathbf{A} \right) (\beta^{i+1} - \mathbf{y}^{i+1}) \geq 0$$

 | Accept update: set $L_{i+1} = \bar{L}$ and $\alpha_i = \bar{\alpha}$;

 | **break**;

end

end

 Terminate if current iterate is approximately stationary:

$$\text{if } \|\mathbf{A}\beta^{i+1} + \mathbf{d} + \lambda \text{sign}(\beta^{i+1})\|_\infty < p\epsilon:$$

 | The algorithm has converged;

 | **break**;

end

end

The ADMM generates a sequence of iterates using approximate dual gradient ascent as follows. The augmented Lagrangian of (27) is defined by

$$\mathcal{L}_\mu(\mathbf{x}, \mathbf{y}, \mathbf{z}) = \frac{1}{2} \mathbf{x}^T \mathbf{A} \mathbf{x} + \mathbf{d}^T \mathbf{x} + \lambda \|\mathbf{y}\|_1 + \mathbf{z}^T (\mathbf{x} - \mathbf{y}) + \frac{\mu}{2} \|\mathbf{x} - \mathbf{y}\|^2$$

for all $\mathbf{x}, \mathbf{y}, \mathbf{z} \in \mathbf{R}^p$; here, $\mu > 0$ is a penalty parameter controlling the emphasis on enforcing feasibility of the primal iterates \mathbf{x} and \mathbf{y} . To approximate the gradient of the dual functional of (27), we alternately minimize the augmented Lagrangian with respect to \mathbf{x} and \mathbf{y} . We then update the dual variable \mathbf{z} using a dual ascent step using this approximate gradient.

Suppose that we have the iterates $(\mathbf{x}^i, \mathbf{y}^i, \mathbf{z}^i)$ after i iterations. To update \mathbf{x} , we take

$$\mathbf{x}^{i+1} = \arg \min_{\mathbf{x} \in \mathbf{R}^p} \mathcal{L}_\mu(\mathbf{x}, \mathbf{y}^i, \mathbf{z}^i) = \arg \min_{\mathbf{x} \in \mathbf{R}^p} \frac{1}{2} \mathbf{x}^T (\mu \mathbf{I} + \mathbf{A}) \mathbf{x} - \mathbf{x}^T (-\mathbf{d} + \mu \mathbf{y}^i - \mathbf{z}^i).$$

Applying the first order necessary and sufficient conditions for optimality, we see that \mathbf{x}^{i+1} must satisfy

$$(\mu \mathbf{I} + \mathbf{A}) \mathbf{x}^{i+1} = -\mathbf{d} + \mu \mathbf{y}^i - \mathbf{z}^i. \quad (28)$$

Thus, \mathbf{x}^{i+1} is obtained as the solution of a linear system. Note that the coefficient matrix $\mu \mathbf{I} + \mathbf{A}$ is independent of the iteration number i ; we take the Cholesky decomposition of $\mu \mathbf{I} + \mathbf{A} = \mathbf{B} \mathbf{B}^T$ during a preprocessing step and obtain \mathbf{x}^{i+1} by solving the two triangular systems given by

$$\mathbf{B} \mathbf{B}^T \mathbf{x}^{i+1} = -\mathbf{d} + \mu \mathbf{y}^i - \mathbf{z}^i.$$

When the generalized elastic net matrix $\mathbf{\Omega}$ is diagonal, or $\mathbf{M} := \mu\mathbf{I} + 2\gamma\mathbf{\Omega}$ is otherwise easy to invert, we can invoke the Sherman-Morrison-Woodbury formula (see [18, Section 2.1.4]) to solve this linear system more efficiently; more details will be provided in Section 2.4. In particular, we see that

$$(\mu\mathbf{I} + 2\gamma\mathbf{\Omega} + 2\mathbf{X}^T\mathbf{X})^{-1} = \mathbf{M}^{-1} - 2\mathbf{M}^{-1}\mathbf{X}^T(\mathbf{I} + 2\mathbf{X}\mathbf{M}^{-1}\mathbf{X}^T)^{-1}\mathbf{X}\mathbf{M}^{-1};$$

computing this inverse only requires computing the inverse of \mathbf{M} and the inverse of the $n \times n$ matrix $\mathbf{I} + 2\mathbf{X}\mathbf{M}^{-1}\mathbf{X}^T$.

Next \mathbf{y} is updated by

$$\mathbf{y}^{i+1} = \arg \min_{\mathbf{y} \in \mathbf{R}^p} \mathcal{L}_\mu(\mathbf{x}^{i+1}, \mathbf{y}, \mathbf{z}^i) = \arg \min_{\mathbf{y}} \lambda \|\mathbf{y}\|_1 + \frac{\mu}{2} \|\mathbf{y} - \mathbf{x}^{i+1} - \mathbf{z}^i/\mu\|^2.$$

That is, \mathbf{y}^{i+1} is updated as the value of the soft thresholding operator of the ℓ_1 -norm at $\mathbf{z}^i/\mu + \mathbf{x}^{i+1}$:

$$\mathbf{y}^{i+1} = S_{\lambda/\mu}(\mathbf{x}^{i+1} + \mathbf{z}^i/\mu). \quad (29)$$

Finally, the dual variable \mathbf{z} is updated using the approximate dual ascent step

$$\mathbf{z}^{i+1} = \mathbf{z}^i + \mu(\mathbf{x}^{i+1} - \mathbf{y}^{i+1}). \quad (30)$$

Following each iteration, we check that the Karush-Kuhn-Tucker conditions for (25) have been approximately satisfied as a stopping criterion. Specifically, we check if the updated iterates $(\mathbf{x}^{i+1}, \mathbf{y}^{i+1}, \mathbf{z}^{i+1})$ have satisfied primal and dual feasibility within relative tolerance of ϵ by checking if the inequalities

$$\begin{aligned} \|\mathbf{x}^{i+1} - \mathbf{y}^{i+1}\| &\leq \epsilon \max\{\|\mathbf{x}^{i+1}\|, \|\mathbf{y}^{i+1}\|\} \\ \mu\|\mathbf{y}^{i+1} - \mathbf{y}^i\| &\leq \epsilon \|\mathbf{y}^{i+1}\|, \end{aligned}$$

respectively, are satisfied. This approach is summarized in Algorithm 6.

It is well-known that the ADMM generates a sequence of iterates which converge linearly to an optimal solution of (25) under certain strong convexity assumptions on f and g and rank assumptions on \mathbf{A} and \mathbf{B} , all of which are satisfied by our problem (27) when $\mathbf{\Omega}$ is positive definite (see, for example, [11, 17, 24, 34]). It follows that the sequence of iterates $\{\mathbf{x}^i, \mathbf{y}^i, \mathbf{z}^i\}$ generated by Algorithm 6 converges to a minimizer of $F(\boldsymbol{\beta})$; that is, $\mathbf{x}^i - \mathbf{y}^i \rightarrow \mathbf{0}$ and $F(\mathbf{x}^i), F(\mathbf{y}^i)$ converge linearly to the minimum value of F . We have the following theorem.

Theorem 2.4 *Suppose $(\mathbf{x}^i, \mathbf{y}^i, \mathbf{z}^i)$ is generated by Algorithm 6. Suppose further that the objective function of (25), $F(\mathbf{x}, \mathbf{y}) = \frac{1}{2}\mathbf{x}^T\mathbf{A}\mathbf{x} + \mathbf{d}^T\mathbf{x} + \lambda\|\mathbf{y}\|_1$, is strongly convex. Then the sequence of iterates satisfies $\mathbf{x}^i - \mathbf{y}^i \rightarrow \mathbf{0}$ and*

$$F(\mathbf{x}^i, \mathbf{y}^i) - F(\mathbf{x}^*, \mathbf{y}^*) \leq \frac{C\|\mathbf{A}\|\|\mathbf{x}^0 - \mathbf{x}^*\|^2}{i} \quad (31)$$

for some constant $C > 0$, where $(\mathbf{x}^*, \mathbf{y}^*)$ is a minimizer of (25).

If F is not strongly convex, then we should expect Algorithm (6) to generate a sequence of iterates that converges sublinearly in value to the optimal value of (13).

2.4 Computational Requirements

To motivate the use of our proposed proximal methods for the minimization of (13), we briefly sketch the computational costs of each of our methods. We will see that for certain choices of regularization parameters, the number of floating point operations needed scales linearly with the size of the data.

We begin by with the computational costs of the proximal gradient method (Algorithms 3 and 2). The computational requirements for the accelerated proximal gradient (Alg. 4 and 5) and alternating direction method of multipliers (Alg. 6) can be calculated in a similar fashion; a full calculation of the complexity of each iteration of each method can be found in Appendix A. The most expensive operation of each iteration of Alg. 3 is the calculation of the gradient: $\nabla f(\boldsymbol{\beta}) = \mathbf{A}\boldsymbol{\beta}$. This requires $\mathcal{O}(np)$ floating point operations

Algorithm 6: Alternating direction method of multipliers for solving (27)

Data: Given initial iterates $\mathbf{x}^0 = \mathbf{y}^0$, step length μ , stopping tolerance ϵ , and maximum number of iterations N .

Result: Solution $\beta^* = \mathbf{x}^* = \mathbf{y}^*$ of (13).

for $i = 0, 1, 2 \dots, N$

 Update \mathbf{x} by (28):

$$(\mu \mathbf{I} + \mathbf{A})\mathbf{x}^{i+1} = -\mathbf{d} + \mu \mathbf{y}^i - \mathbf{z}^i;$$

 Update \mathbf{y} using soft thresholding (29):

$$\mathbf{y}^{i+1} = S_{\lambda/\mu}(\mathbf{x}^{i+1} + \mathbf{z}^i/\mu);$$

 Update \mathbf{z} using approximate dual ascent (30):

$$\mathbf{z}^{i+1} = \mathbf{z}^i + \mu(\mathbf{x}^{i+1} - \mathbf{y}^{i+1});$$

 Test stopping criterion:

if $\|\mathbf{x}^{i+1} - \mathbf{y}^{i+1}\| \leq \epsilon \max\{\|\mathbf{x}^{i+1}\|, \|\mathbf{y}^{i+1}\|\}$ and $\mu\|\mathbf{y}^{i+1} - \mathbf{y}^i\| \leq \epsilon\|\mathbf{y}^{i+1}\|$

 The algorithm has converged;

break;

end

end

Method	Total Flops	Method	Total Flops
PG	$\mathcal{O}(np/\epsilon)$	APG	$\mathcal{O}(np/\sqrt{\epsilon})$
ADMM	$\mathcal{O}(n^2p/\epsilon)$	LARS	$\mathcal{O}(mnp + m^3)$

Table 1: Upper bounds on total number of floating point operations required to calculate an ϵ -suboptimal solution (PG, APG, ADMM) or solution containing m nonzero entries (LARS) using of (13) diagonal regularization matrix $\mathbf{\Omega}$.

(flops) if the regularization matrix $\mathbf{\Omega}$ is a diagonal matrix (and $\mathcal{O}(p^2)$ flops for unstructured $\mathbf{\Omega}$). On the other hand, Theorem 2.2 implies that Alg. 3 and 2 generate an ϵ -suboptimal solution of (13) within $\mathcal{O}(1/\epsilon)$ iterations. Putting everything together, we see that Alg. 3 and 2 yield ϵ -suboptimal solutions using at most $\mathcal{O}(np/\epsilon)$ flops if $\mathbf{\Omega}$ is a diagonal matrix. Performing similar calculations for Alg. 4, 5, and 6 yields the total complexity estimates for each method, found in Table 1.

The complexity estimates found in Table 1 establish that the accelerated proximal gradient method is more efficient for solution of (13) than least angle regression if

$$\frac{np}{\sqrt{\epsilon}} \ll mnp + m^3, \quad (32)$$

where m is the number of nonzero entries of the optimal solution β^* . In particular, if m is moderately large, e.g., $m = c(np)^{1/3}$ for sufficiently large c , APG is significantly more efficient for solution of (13) than LARS. In practice, this improvement in computational complexity is large when p is large (e.g., $p > 1000$). Section 3 provides a detailed empirical analysis of the computational complexity of these algorithms for solving (13).

2.5 Convergence analysis of the block coordinate descent method

In this section, we investigate the convergence properties of our block coordinate descent method (Algorithm 1). Our two main results, Theorem 2.5 and Theorem 2.6, are specializations of standard results for alternating minimization algorithms; we provide proofs of these results as appendices.

We first note that the Lagrangian $\mathcal{L} : \mathbf{R}^K \times \mathbf{R}^p \times \mathbf{R} \times \mathbf{R}^{j-1} \rightarrow \mathbf{R}$ of (2) is given by

$$\begin{aligned} \mathcal{L}(\boldsymbol{\theta}, \boldsymbol{\beta}, \psi, \mathbf{v}) = & \|\mathbf{Y}\boldsymbol{\theta} - \mathbf{X}\boldsymbol{\beta}\|^2 + \gamma\boldsymbol{\beta}^T \boldsymbol{\Omega}\boldsymbol{\beta} + \lambda\|\boldsymbol{\beta}\|_1 \\ & + \psi(\boldsymbol{\theta}^T \mathbf{Y}^T \mathbf{Y} \boldsymbol{\theta} - n) + \mathbf{v}^T \mathbf{U} \boldsymbol{\theta}, \end{aligned}$$

where $\mathbf{U}^T = (\mathbf{Y}^T \mathbf{Y} \boldsymbol{\theta}_1, \mathbf{Y}^T \mathbf{Y} \boldsymbol{\theta}_2, \dots, \mathbf{Y}^T \mathbf{Y} \boldsymbol{\theta}_{j-1})$. Note that the Lagrangian is *not* a convex function in general. However, \mathcal{L} is the sum of the (possibly) nonconvex quadratic $\|\mathbf{Y}\boldsymbol{\theta} - \mathbf{X}\boldsymbol{\beta}\|^2 + \psi(\boldsymbol{\theta}^T \mathbf{Y}^T \mathbf{Y} \boldsymbol{\theta} - n) + \gamma\boldsymbol{\beta}^T \boldsymbol{\Omega}\boldsymbol{\beta} + \mathbf{v}^T \mathbf{U} \boldsymbol{\theta}$ and the convex nonsmooth function $\lambda\|\boldsymbol{\beta}\|_1$; therefore, \mathcal{L} is subdifferentiable, with subdifferential at $(\boldsymbol{\beta}, \boldsymbol{\theta})$ given by the sum of the gradient of the smooth term at $(\boldsymbol{\beta}, \boldsymbol{\theta})$ and the subdifferential of the convex nonsmooth term at $(\boldsymbol{\beta}, \boldsymbol{\theta})$.

We now provide our first convergence result, specifically, that Algorithm 1 generates a convergent sequence of function values.

Theorem 2.5 *Suppose that the sequence of iterates $\{(\boldsymbol{\theta}^i, \boldsymbol{\beta}^i)\}_{i=0}^\infty$ is generated by Algorithm 1. Then the sequence of objective function values $\{F(\boldsymbol{\theta}^i, \boldsymbol{\beta}^i)\}_{i=0}^\infty$ defined by $F(\boldsymbol{\theta}, \boldsymbol{\beta}) := \|\mathbf{Y}\boldsymbol{\theta} - \mathbf{X}\boldsymbol{\beta}\|^2 + \gamma\boldsymbol{\beta}^T \boldsymbol{\Omega}\boldsymbol{\beta} + \lambda\|\boldsymbol{\beta}\|_1$ is convergent.*

We include a proof of Theorem 2.5 in Appendix B.

We also have the following theorem, which establishes that every convergent subsequence of $\{(\boldsymbol{\theta}^i, \boldsymbol{\beta}^i)\}_{i=1}^\infty$ converges to a stationary point of (2).

Theorem 2.6 *Let $\{(\boldsymbol{\theta}^i, \boldsymbol{\beta}^i)\}_{i=1}^\infty$ be the sequence of points generated by Algorithm 1. If $\{(\boldsymbol{\theta}^{i_\ell}, \boldsymbol{\beta}^{i_\ell})\}_{\ell=1}^\infty$ is a convergent subsequence of $\{(\boldsymbol{\theta}^i, \boldsymbol{\beta}^i)\}_{i=1}^\infty$ with limit $(\boldsymbol{\theta}^*, \boldsymbol{\beta}^*)$ then $(\boldsymbol{\theta}^*, \boldsymbol{\beta}^*)$ is a stationary point of (2): $(\boldsymbol{\theta}^*, \boldsymbol{\beta}^*)$ is feasible for (2) and there exists $\psi^* \in \mathbf{R}$ and $\mathbf{v}^* \in \mathbf{R}^{j-1}$ such that $\mathbf{0} \in \partial\mathcal{L}(\boldsymbol{\theta}^*, \boldsymbol{\beta}^*, \psi^*, \mathbf{v}^*)$, where $\partial\mathcal{L}(\boldsymbol{\theta}, \boldsymbol{\beta}, \psi, \mathbf{v})$ denotes the subdifferential of the Lagrangian function \mathcal{L} with respect to the primal variables $(\boldsymbol{\theta}, \boldsymbol{\beta})$.*

A proof of Theorem 2.6 can be found in Appendix C.

3 Numerical Analysis

We next compare the performance of our proposed approaches with standard methods for penalized discriminant analysis in several numerical experiments. In particular, we compare the implementations of the block coordinate descent method Algorithm 1, where each discriminant direction $\boldsymbol{\beta}$ is updated using either the proximal gradient method with constant step size, Algorithm 3 (PG), the proximal gradient method with backtracking line search, Algorithm 2 (PGB), the accelerated proximal method with constant step size, Algorithm 4 (APG), the accelerated proximal method with backtracking, Algorithm 5 (APGB), and the alternating direction method of multipliers, Algorithm 6, (ADMM), with the least angle regression based algorithm (LARS) for solving the sparse optimal scoring problem proposed in [8].

3.1 Gaussian data

We first perform simulations investigating efficacy of our heuristics for classification of Gaussian data. In each experiment, we generate data consisting of p -dimensional vectors from one of K multivariate normal distributions. Specifically, we obtain training observations corresponding to the i th class, $i = 1, 2, \dots, K$, by sampling 25 observations from the multivariate normal distribution with mean $\boldsymbol{\mu}_i \in \mathbf{R}^p$ satisfying

$$[\boldsymbol{\mu}_i]_j = \begin{cases} 0.7, & \text{if } 100(i-1) < j \leq 100i \\ 0, & \text{otherwise,} \end{cases} \quad (33)$$

for all $j = 1, 2, \dots, p$, and covariance matrix $\boldsymbol{\Sigma} \in \mathbf{R}^{p \times p}$ chosen so that all features are correlated with $\Sigma_{ij} = r$ for all $i \neq j$ and $\Sigma_{ii} = 1$ for all i . We conduct the experiment for all $K \in \{2, 4\}$, $r \in \{0, 0.1, 0.5, 0.9\}$. For each experiment, we sample 250 testing observations from each class in the same manner as the training data. We set $p = 1500$ in each simulation. For each (K, r) pair we generate 20 data sets and use nearest centroid

classification following projection onto the span of the discriminant directions calculated using Algorithm 1 and PG, PGB, APG, APGB, ADMM, or LARS to solve (13), or SZVD.

The sparse discriminant analysis heuristics require training of the regularization parameters γ , $\mathbf{\Omega}$, and λ . In all experiments, we set $\gamma = 10^{-3}$ and $\mathbf{\Omega}$ to be the $p \times p$ identity matrix $\mathbf{\Omega} = \mathbf{I}$. We train the remaining parameter λ using 5-fold cross validation. Specifically, we choose λ from a set of potential λ of the form $\bar{\lambda}/2^c$ for $c = 9, 8, 7, \dots, -1, -2, -3$ and $\bar{\lambda}$ chosen so that the problem has nontrivial solution for all considered λ . Note that (18) has optimal solution given by $\beta^* = \mathbf{A}^{-1}\mathbf{d}$ if we set $\lambda = 0$; this implies that choosing

$$\bar{\lambda} = \frac{(\beta^*)^T \mathbf{d} - \frac{1}{2}(\beta^*)^T \mathbf{A} \beta^*}{\|\beta^*\|_1} \quad (34)$$

ensures that there exists at least one solution β^* with value strictly less than zero. We choose the value of λ with fewest average number of misclassification errors over training-validation splits amongst all λ which yield discriminant vectors containing at most 15% nonzero entries. Note that we could have applied other resampling methods, e.g., boot strapping, to train the regularization parameter using the same criteria with minimal changes to the experiment. The LARS algorithm terminates after a solution with desired maximum cardinality is identified; we apply 5-fold cross validation to select this maximum cardinality from 13 equally spaced potential values from $0.025qp$ to $0.5qp$. We terminate each proximal algorithm in the inner loop after 1000 iterations or a 10^{-5} suboptimal solution is obtained; the outer block coordinate descent loop is stopped after a maximum number of 250 iterations or a 10^{-3} suboptimal solution has been found. The augmented Lagrangian parameter $\mu = 2$ was used in all experiments in the ADMM method. We use the value of $\bar{L} = 0.25$ for the initial estimate of the Lipschitz constant and $\eta = 1.25$ for the scalar multiplier in the backtracking line search. These stopping criteria and parameter choices were chosen empirically in order to yield accurate classifiers using a minimal number of iterations; in particular, using modest stopping tolerances limits the number of iterations performed, which tends to limit overfitting in practice.

We also include the Sparse Zero-Variance Discriminant Analysis (SZVD) method proposed in [2] in our comparisons. We train the regularization parameter γ in SZVD in a fashion similar to that above. We set the maximum value of the regularization parameter γ to

$$\bar{\gamma} = \frac{\hat{\beta}^T \mathbf{B} \hat{\beta}}{\|\hat{\beta}\|_1}, \quad (35)$$

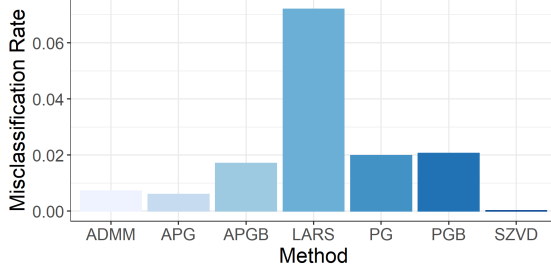
where $\hat{\beta}$ is the optimal solution of the unpenalized SZVD problem and \mathbf{B} is the sample between-class covariance matrix of the training data. We choose γ from the exponentially spaced grid $\bar{\gamma}/2^c$ for $c = 9, 8, \dots, -2, -3$ using 5-fold cross-validation; this approach is consistent with that in [2]. We select the value of γ which minimizes misclassification error amongst all sets of discriminant vectors with at most 35% nonzero entries; this acceptable sparsity threshold is chosen to be higher than that in the SOS experiments, due to the tendency of SZVD to misconverge to the trivial all-zero solution for large values of γ . We stop SZVD after a maximum of 1000 iterations or a solution satisfying the stopping tolerance of 10^{-5} is obtained. We use the augmented Lagrangian penalty parameter $\beta = 5$ in SZVD in all experiments. All simulations were conducted using R version 3.5.0 and our heuristics are implemented in R as the package **accSDA** (see [12]).

Figures 1, 2, 3, 4, 5, and 6 summarize the results of these experiments; complete tables of numerical results can be found in the electronic supplemental materials². From these simulations, we see that the classical solution of the SOS problem using LARS tends to use fewer predictor variables than the proximal methods (Fig. 3 and 4), often at a cost of significantly lower prediction accuracy (Fig. 1 and 2). The accelerated proximal gradient method tend to require significantly less computation-time than LARS (see Fig. 5), with fewer classification errors. This agrees with the improvement in computational complexity predicted by (32). We further investigate this phenomena in the following sections.

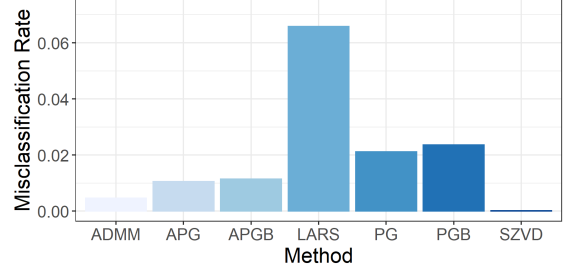
3.2 Convergence Experiments

The empirical results of Section 3.1 suggest that the use of our proposed proximal methods (PG, PGB, APG, APGB, ADMM) for solution of Subproblem (13) can lead to significant improvement in terms of

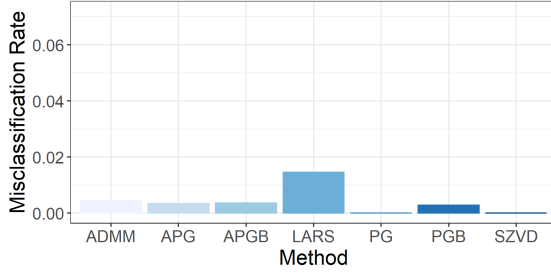
²Available from <https://bpames.people.ua.edu/uploads/3/9/0/0/39000767/asda-paper-esm.zip>



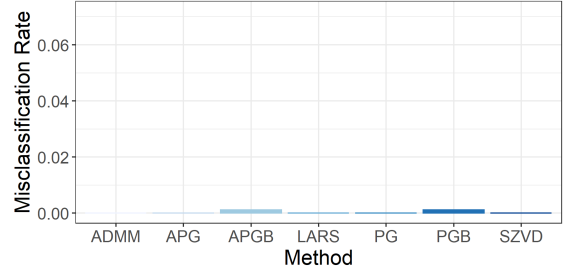
(a) $K = 2, r = 0$



(b) $K = 2, r = 0.1$



(c) $K = 2, r = 0.5$



(d) $K = 2, r = 0.9$

Figure 1: Average out-of-sample misclassification rate for 2-class Gaussian data with class means defined by (33) and covariance vector Σ for given values of r . For each data set, we use nearest centroid classification following projection onto discriminant vectors given by the sparse zero variance method (SZVD) or optimal scoring vectors calculated using the proximal gradient method with constant stepsize (PG), with backtracking line search (PGB), accelerated proximal method with constant stepsize (APG) and backtracking line search (APGB), alternating direction method of multipliers (ADMM), and least angle regression (LARS). In all experiments, $n_{train} = 50$ and $n_{test} = 500$. Classifiers built using LARS consistently misclassify more testing data than other methods.

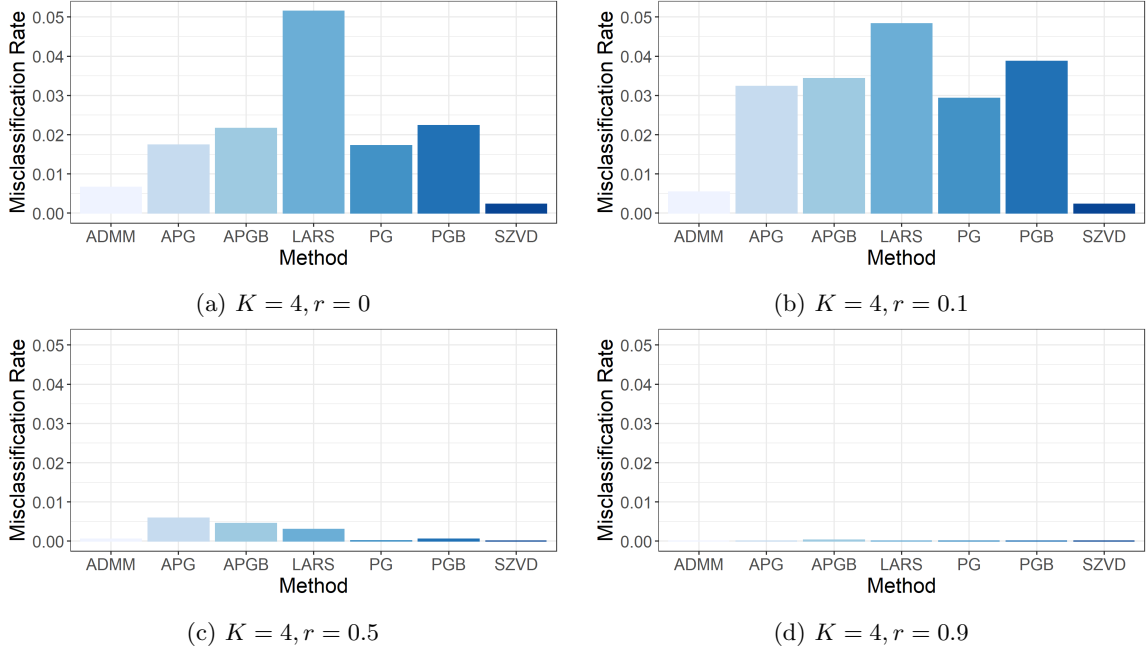


Figure 2: Average out-of-sample misclassification rate using discriminant vectors calculated using APG, APGB, PG, PGB, ADMM, SZVD, and LARS for 4-class Gaussian data with class means defined by (33) and covariance vector Σ for given values of r . In all experiments, $n_{train} = 100$ and $n_{test} = 1000$.

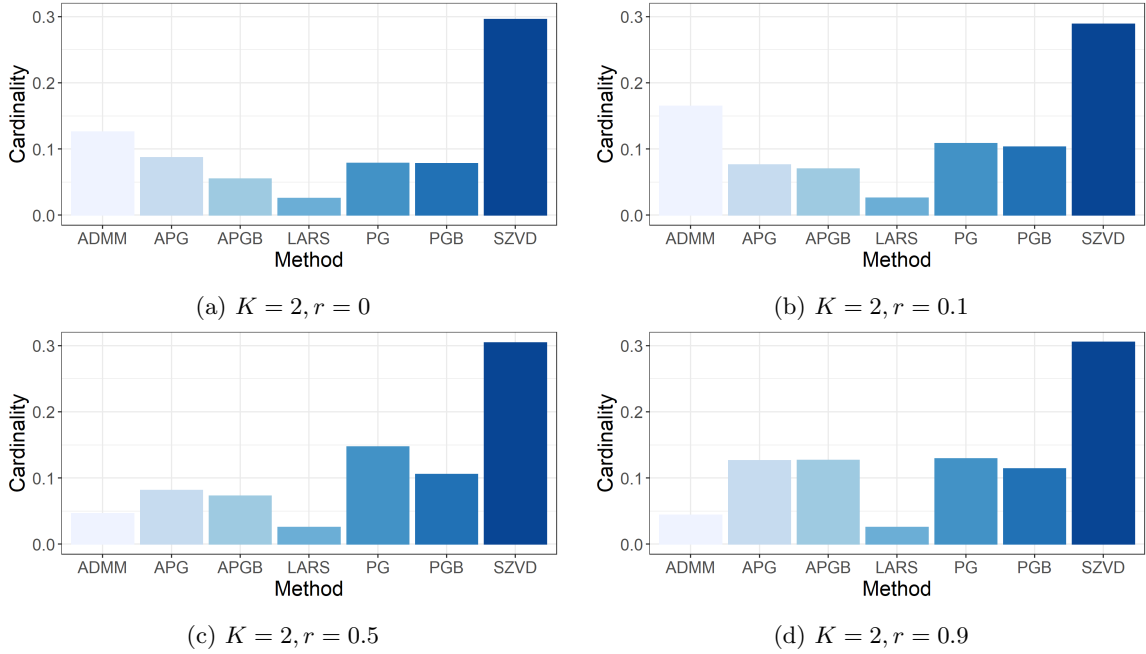


Figure 3: Average fraction of nonzero entries of discriminant vectors and optimal scoring vectors calculated using APG, APGB, PG, PGB, ADMM, SZVD, and LARS for classifying 2-class Gaussian data with mean-vectors defined by (33) and covariance vector Σ for given values of r .

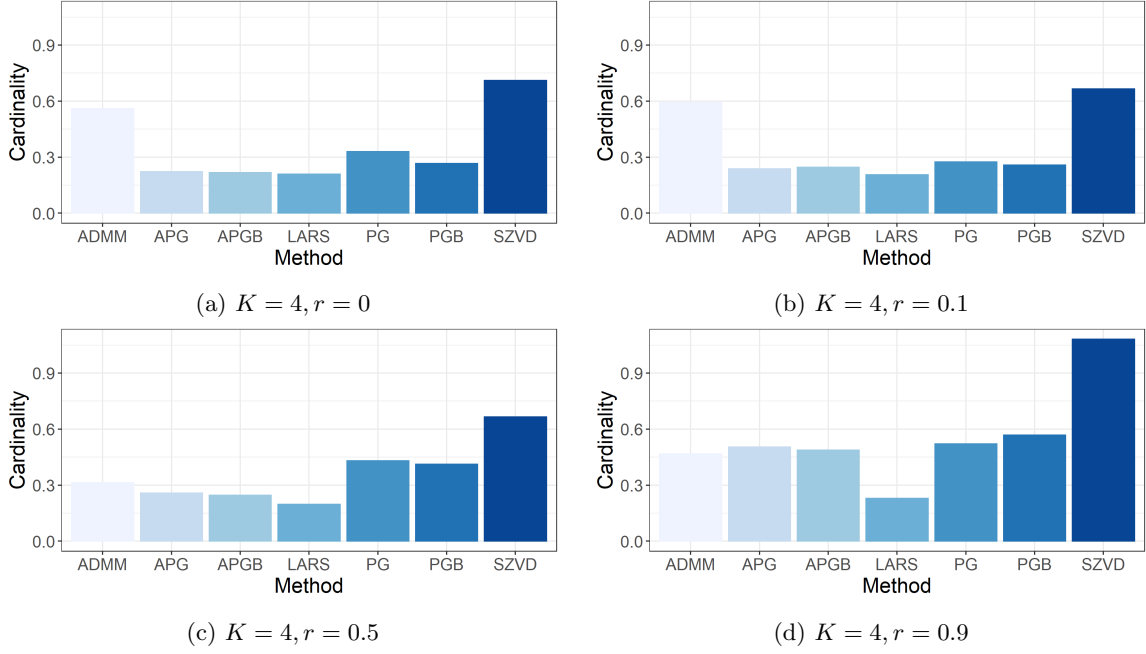


Figure 4: Average fraction of nonzero entries of discriminant vectors and optimal scoring vectors calculated using APG, APGB, PG, PGB, ADMM, SZVD, and LARS for classifying 4-class Gaussian data with mean-vectors defined by (33) and covariance vector Σ for given values of r .

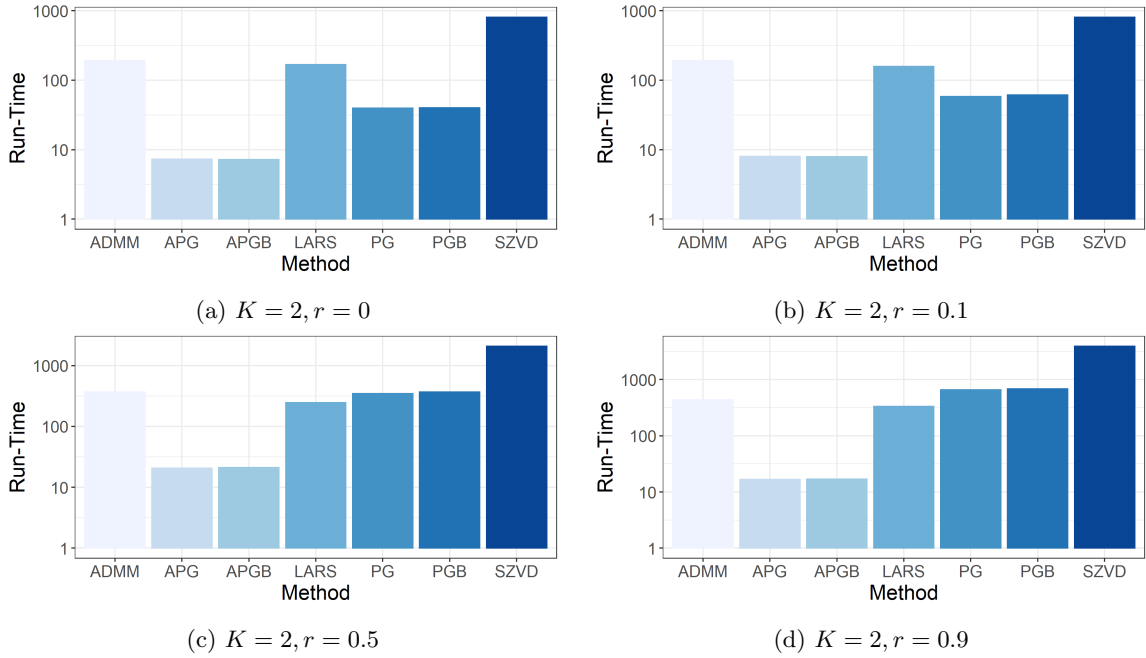


Figure 5: Average run-time for calculation of discriminant vectors and optimal scoring vectors using APG, APGB, PG, PGB, ADMM, SZVD, and LARS for classifying 2-class Gaussian data with mean-vectors defined by (33) and covariance vector Σ for given values of r .

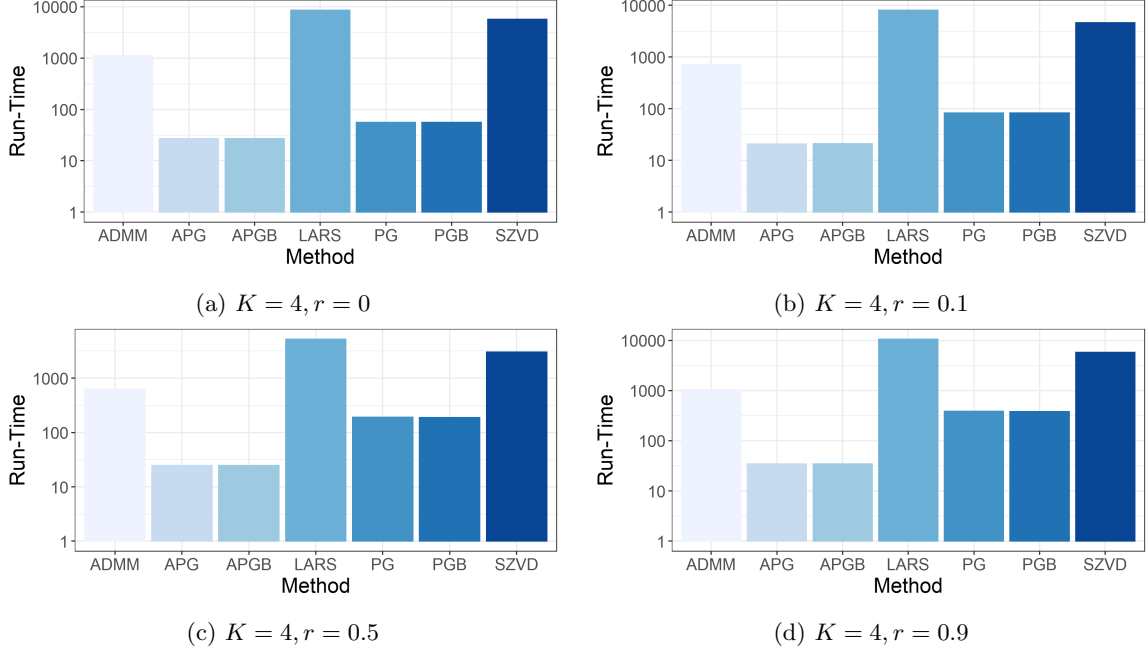


Figure 6: Average run-time for calculation of discriminant vectors and optimal scoring vectors using APG, APGB, PG, PGB, ADMM, SZVD, and LARS for classifying 4-class Gaussian data with mean-vectors defined by (33) and covariance vector Σ for given values of r . LARS consistently requires more time than the proximal methods when $K=4$.

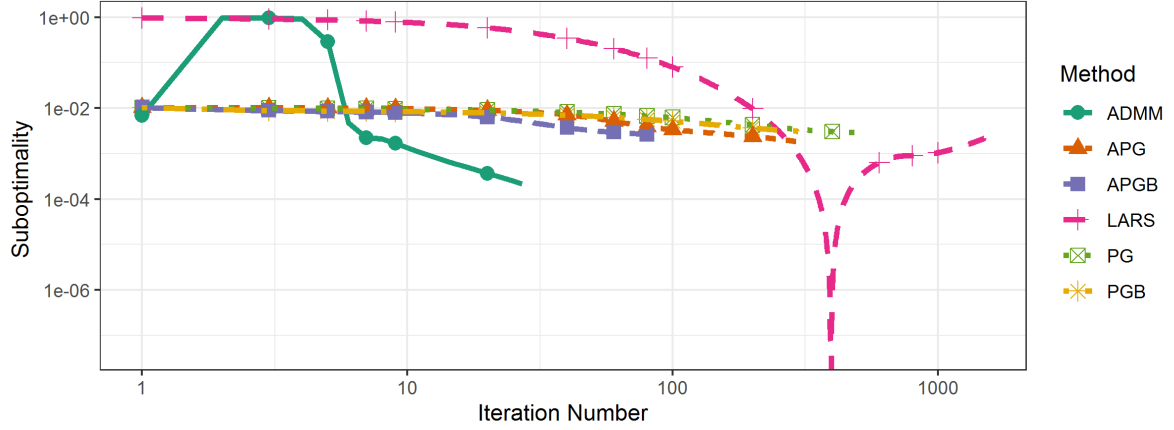
classification accuracy and overall run-time over the least angle regression algorithm. To further illustrate this improvement, we performed a series of experiments investigating the behaviour of the objective function of (2) during each iteration of these methods.

We generated random data sets with observations sampled from one of two normal distributions, $N(\mu_1, \Sigma)$ or $N(\mu_2, \Sigma)$. Specifically, we sampled $n=200$ training observations from each of the p -dimensional multivariate Gaussian distributions for $p=2000$ with mean vectors μ_1 and $\mu_2 \in \mathbf{R}^p$, respectively, satisfying

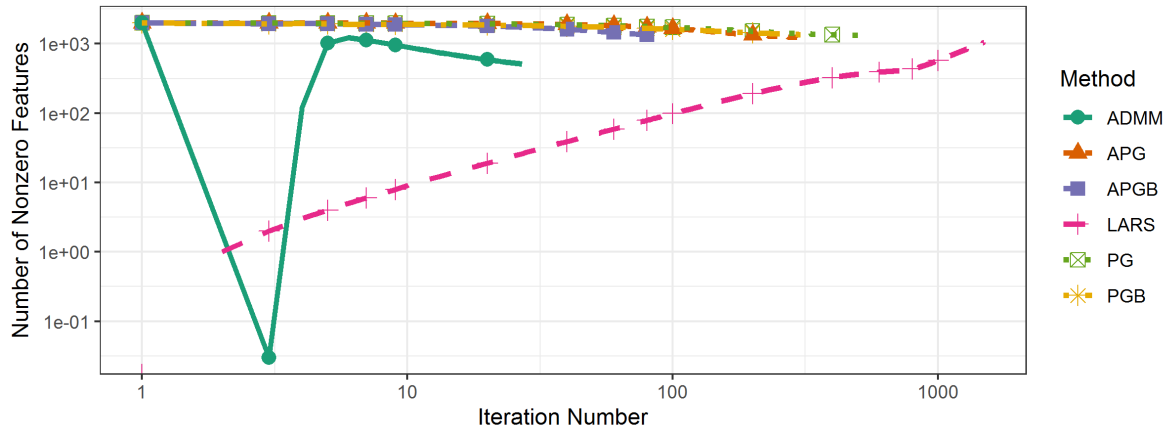
$$[\mu_i]_j = \begin{cases} 0.7, & \text{if } [p/3](i-1) < j \leq [p/3]i \\ 0, & \text{otherwise,} \end{cases} \quad (36)$$

for all $j=1, 2, \dots, p$, and covariance matrix $\Sigma \in \mathbf{R}^{p \times p}$ constructed as Section 3.1 with $r=0.75$. For each data set, we train nearest centroid classifiers using discriminant vectors obtained by approximately solving (2) with each method used above (PG, PGB, APG, APGB, ADMM, LARS) to solve (13). We stop each method after either 2500 iterations have been performed or the stopping condition is met with tolerance $10^{-4}/\sqrt{p}$. We use regularization parameters $\gamma=10^{-3}$, $\Omega=\mathbf{I}$ and we set $\lambda=0.05\bar{\lambda}$, where $\bar{\lambda}$ is given by (34); we stop LARS when a solution with cardinality matching the maximum cardinality of all other methods is found. We use augmented Lagrangian parameter $\mu=2$ in ADMM. We use the parameters $\bar{L}=0.25$ and $\eta=1.25$ in the back tracking line search. Note that these stopping conditions are more strict than those used in the previous section (Sect. 3.1); we use these stopping criteria to ensure that a large number of iterations are performed in order to obtain a clearer picture of the convergence properties of the various algorithms. We repeated the process 100 times for each method and data set to control for natural variation in computation time; each algorithms will generate the same sequence of iterates and solution each time (up to sign changes due to random initialization of θ). We validate performance of our classifiers using balanced sets of 200 testing observations sampled from $N(\mu_1, \Sigma)$ or $N(\mu_2, \Sigma)$.

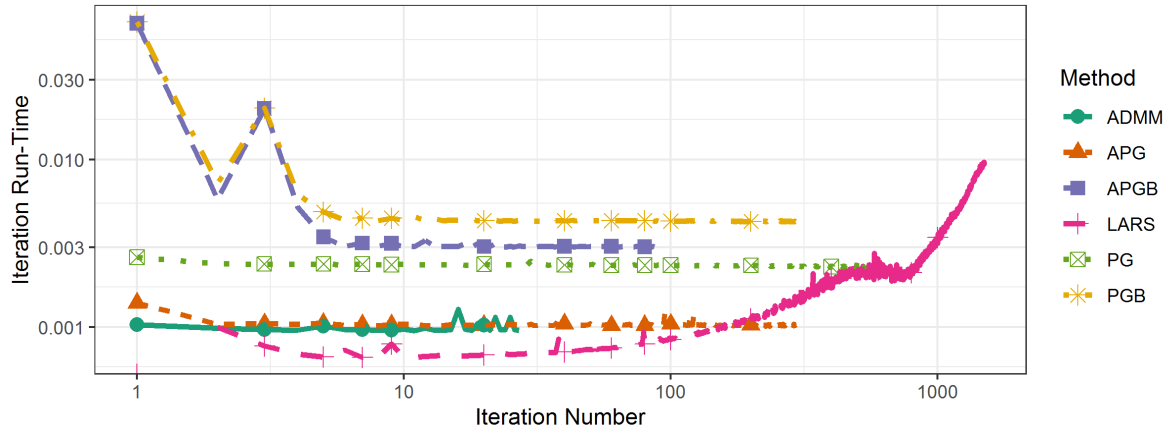
We chose these data sets to isolate the relationship between the performance of our proposed algorithms for solving (13) and the overall performance of the proposed block coordinate descent method and nearest centroid classification. In the $K=2$ class case, we calculate exactly one discriminant and scoring vector



(a) Difference of objective value and optimal value



(b) Number of Nonzero Features



(c) Iteration Run-time

Figure 7: Objective value, cardinality of iterate, and iteration run-time averaged over 100 Gaussian data sets. We note that ADMM converges in the fewest number of iterations, followed by APG; LARS requires the most iterations and has more expensive iterations.

pair (β, θ) . Consequently, we expect the block coordinate descent method to converge after exactly one full iteration in the absence of rounding error. Indeed, the optimal solution of (3) is given by the projection of any vector θ not in the span of the all-ones vector \mathbf{e} onto the set

$$\left\{ \theta \in \mathbf{R}^k : \theta^T \mathbf{Y}^T \mathbf{Y} \theta = n, \theta^T \mathbf{Y}^T \mathbf{Y} \mathbf{e} = 0 \right\};$$

this is equivalent to the optimal solution given by Lemma 2.1. This solution is uniquely defined (up to sign) and is obtained after the initial θ update if the initial solution θ is not a scalar multiple of \mathbf{e} . This suggests that Algorithm 1 will converge after exactly one iteration if we solve (13) exactly. In practice, we may require multiple iterations of Algorithm 1 depending on the relative stopping tolerances of Algorithm 1 and the method used to solve (13); we terminate the block coordinate descent method after one iteration in these experiments.

We recorded the objective value of (13) and the cardinality of the current iterate β^i following the t th iteration of each algorithm for each method and data set, as well as the run-time of the t th iteration. We recorded the value of the augmented Lagrangian function for the ADMM, instead of the objective function value, to indicate the trade-off between optimizing the objective and forcing feasibility ($\mathbf{x} = \mathbf{y} = \beta$) of the split decision variables \mathbf{x} and \mathbf{y} . We also recorded the cardinality and number of misclassification errors of each scoring and discriminant vector pairs calculated by each method. The results of these experiments are summarized in Figure 7. All experiments were performed on a standard node of the University of Alabama’s research computing cluster (UAHPC) using Matlab 2019a; the Matlab implementation of Algorithm 1 can be obtained from https://github.com/gumeo/accSDA_matlab.

It is apparent from the results of these simulations that iterations of LARS are significantly more expensive than those of the proximal methods when the cardinality of the iterate is relatively large. The per-iteration cost of LARS tends to increase since LARS is an active set method and gradually adds elements to the active set each iteration; the computational complexity is an increasing function of iteration number due to this corresponding increase in cardinality each iteration. On the other hand, the per-iteration cost of each proximal method is largely consistent across iterations. The ADMM tended to terminate in fewer iterations and yield sparser solutions than the other proximal methods; the per-iteration cost of the ADMM is also less than (or comparable to) the other proximal methods in all trials. The cardinality of iterates generated by ADMM also decreased much more quickly than those generated by the other proximal methods; this may be due to the fact that the soft thresholding operator is applied directly to the iterate \mathbf{y}^i , rather than following a gradient step applied to the previous iterate or a weighted average of the previous two iterates as in the proximal gradient and accelerated gradient methods.

These trials also suggest some modest value in the use of back tracking line searches. In each set of trials, the proximal gradient methods with back tracking line search terminated in fewer iterations than with a constant step size. However, the additional cost of performing the line search frequently caused the overall computational time of the back tracking methods to exceed that of the constant step size methods. This additional cost observed here is more dramatic than that observed in Section 3.1. We remind the reader that the reported computation time for the experiments of Section 3.1 includes all computation to perform cross validation to train the regularization parameter λ ; the discrepancy between the timing results in Section 3.1 and here highlights a potential sensitivity of Algorithm 1 to choice of λ , variation in training data (in this case with respect to training and validation splits in the cross validation scheme), and computing environment (R versus Matlab).

3.2.1 Differences between discriminant vectors due to algorithm choice.

At this point, we should note that the subproblem (13) is strongly convex by the choice of regularization parameter $\Omega = \mathbf{I}$ in all experiments considered so far. As a consequence, (13) has a *unique* solution. One would naively expect Algorithm 1 to generate the same discriminant vector regardless of choice of algorithm for solving (13) if all other input parameters are chosen consistently. However, this is not observed in practice. We can see from Figure 7 that the compared algorithms generate different sequences of iterates whose limit is the unique optimal solution of (13). We terminate each algorithm prematurely at a suboptimal solution, which varies based on our choice of algorithm.

To illustrate this phenomena, we recorded and plotted the iterates generated by Algorithm 1 using APG and ADMM with $\mu = 2$; we restricted our analyses to these methods to simplify our figures and similar

behaviour would be observed using other algorithms for solving (13). We sampled a balanced training set of $n = 200$ observations of dimension $p = 250$ from $N(\boldsymbol{\mu}_1, \boldsymbol{\Sigma})$ and $N(\boldsymbol{\mu}_2, \boldsymbol{\Sigma})$, where $\boldsymbol{\mu}_i$ is defined according to (36) and $\boldsymbol{\Sigma}$ is constructed as in the previous sections. We recorded the iterates $\boldsymbol{\beta}^i$ generated by each of APG and ADMM (with $\mu = 2$) following $i = 10, 100, 1000, 10000$ iterations for solving (13) with regularization parameters $\gamma = 10^{-3}$, $\boldsymbol{\Omega} = \mathbf{I}$, and $\lambda = 0.05\bar{\lambda}$. We plot these discriminant vectors in Figure 8. Note that the calculated discriminant vectors are qualitatively similar but still differ significantly, particularly in cardinality. Specifically, the discriminant vectors generated by ADMM are much sparser than those calculated by APG, particularly early in the iterative process. This suggests that ADMM is converging to the unique optimal solution of (13) more quickly than APG for this particular data set and choice of augmented Lagrangian penalty parameter μ ; we investigate the sensitivity of ADMM to the choice of μ further in Section 3.6.1. However, we should also note that both methods converge to an identical solution within 10000 iterations, and the observed iterates after 1000 iterations are nearly indistinguishable.

3.3 Scaling Experiments

We next performed a series of simulations to investigate the relationship between performance of our algorithms and the number of features in the underlying data set. For each

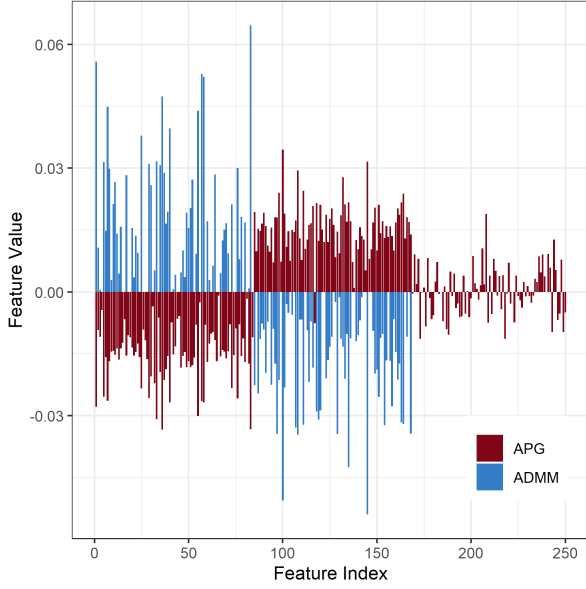
$$p \in \{250, 300, \dots, 500, 600, \dots, 1000, 1250, \dots, 2500, 3000, \dots, 4500\},$$

we sample 100 data sets, containing two classes drawn from the Gaussian distributions as described in Section 3.1. For each value of p , we sample $\lceil p/10 \rceil$ training and testing observations from each class. Items in each class are sampled from a multivariate Gaussian distribution with means $\boldsymbol{\mu}_1, \boldsymbol{\mu}_2 \in \mathbf{R}^p$ defined by (36). Both class distributions have covariance matrix $\boldsymbol{\Sigma}$ having diagonal entries equal to 1 and off-diagonal entries equal to 0.75.

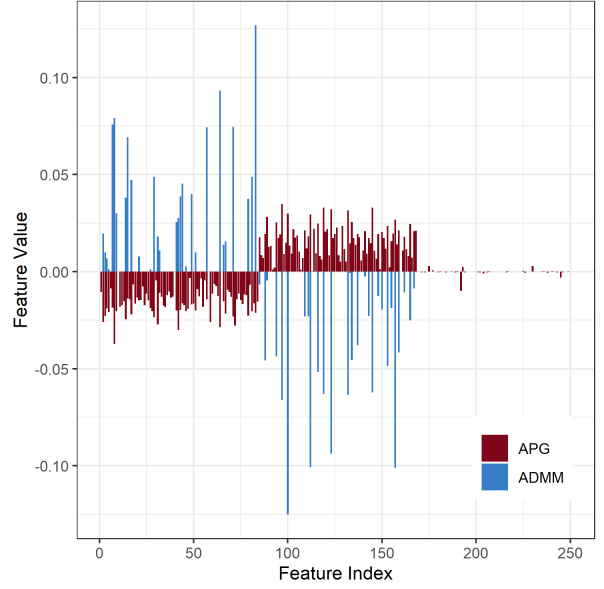
We apply nearest centroid classification following projection onto the approximate solution of (2) given by the proximal gradient method, accelerated proximal gradient method (with and without backtracking line search) (PG, PGB, APG, APGB), alternating direction method of multipliers (ADMM), and least angle regression method (LARS). We perform exactly one full iteration of the block coordinate descent method (Algorithm 1) for each $\boldsymbol{\beta}$ -subproblem solver; as before, we should expect Algorithm 1 to terminate after one full iteration, since the optimal choice of $\boldsymbol{\theta}$ is obtained in the first iteration (in the absence of numerical error). We choose the regularization parameters in (2) to be $\gamma = 10^{-3}$, $\boldsymbol{\Omega} = \mathbf{I}$, and $\lambda = 0.25\bar{\lambda}$, where $\bar{\lambda}$ is defined as in (34); we used the augmented Lagrangian penalty parameter $\mu = 2$ in ADMM. We terminated the proximal methods when their stopping condition is met with tolerance 10^{-4} or 5000 subproblem iterations have been performed; we used backtracking parameters $\bar{L} = 0.25$ and $\eta = 1.25$ in each run; we use a less strict stopping tolerance than earlier analyses to minimize the number of iterations performed when p is large, and, thus, decreasing run-time of the experiment. The LARS heuristic was terminated after a solution was obtained containing the number of nonzero elements of the densest solution returned by the other five methods for each data set. All experiments were conducted on UAHPC using Matlab 2019a.

Figure 9 summarizes the results of these simulations. We note that the accelerated proximal gradient and alternating direction method of multipliers consistently outperforms the traditional LARS method in terms of run-time, number of iterations performed, and classification error. We also note that no methods calculate discriminant vectors which lead to classification error for all $p > 1000$. In particular, these methods require significantly fewer iterations and terminate in less time than LARS for large p . The approximate slopes of the plots of average run-times indicate that this phenomena will only be amplified as we increase p further, since the slope of the curve for LARS exceeds that of APG, APGB, and ADMM. This largely agrees with the phenomena predicted by the operation counts discussed in Section 2.4. On the other hand, the proximal gradient methods (PG, PGB) typically do not converge within the maximum number of iterations, which undermines any improvements to computational complexity due to their relatively inexpensive iterations.

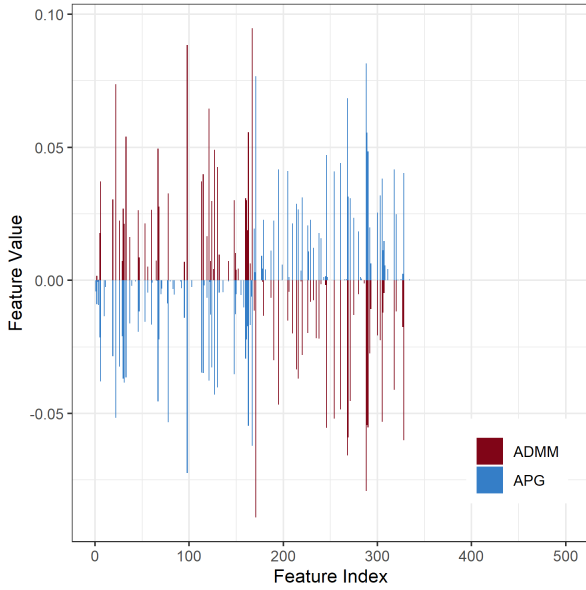
We should note that we expect the cardinality of our obtained discriminant vectors to increase as a function of p , since the size of the blocks of entries with elevated values in the class-means $\boldsymbol{\mu}_1$ and $\boldsymbol{\mu}_2$ grows linearly with p . This agrees with the plotted curves in Figure 9c. This also explains the linear increase in number of iterations before termination of the LARS method, since the number of iterations depends on the desired number of nonzero entries; in turn, this, along with increase in per-iteration cost as p



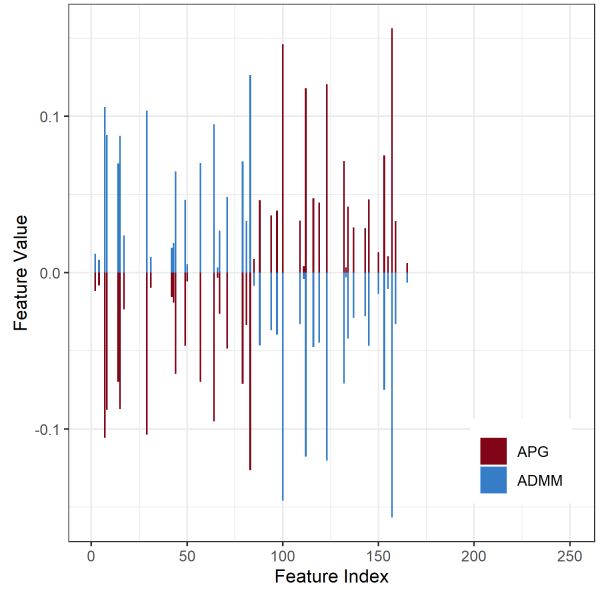
(a) After 10 iterations



(b) After 100 iterations

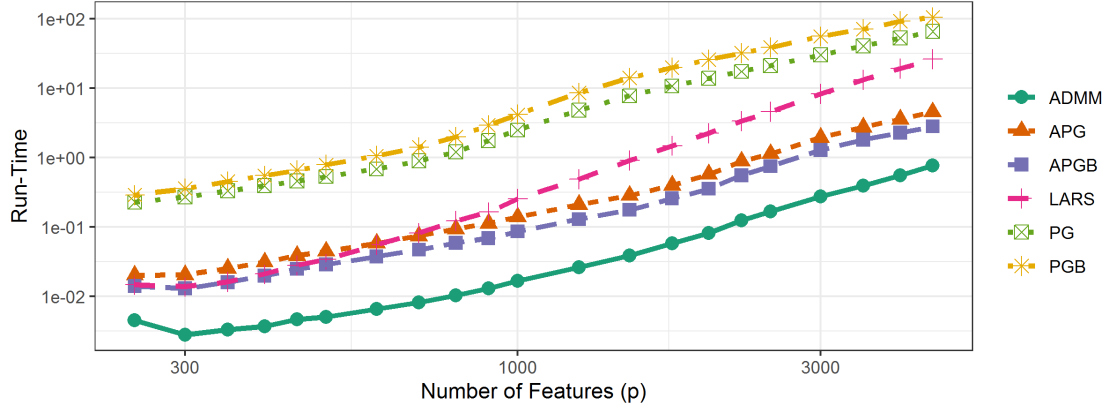


(c) After 1000 iterations

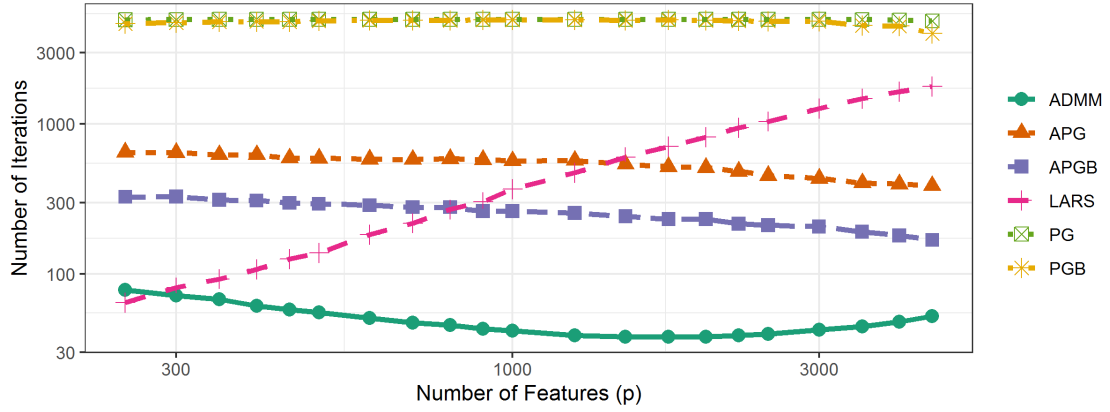


(d) After 10000 iterations

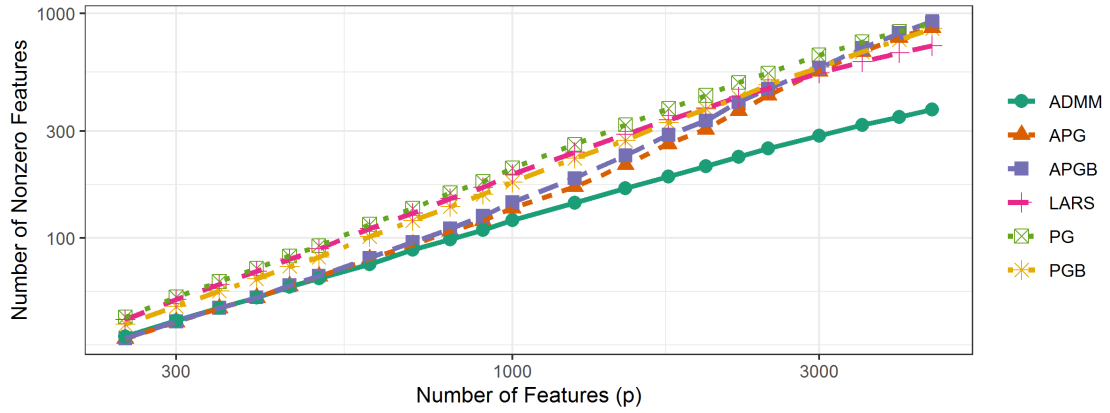
Figure 8: Bar plots of discriminant vectors β calculated using ADMM and APG following 10, 100, 1000, and 10000 iterations. Signs of the discriminant vectors are reversed for clarity. ADMM discriminant vectors are considerably more sparse than those generated by APG in first few hundred iterations, but both methods converge to identical solutions within 10000 iterations.



(a) Time



(b) Number of iterations



(c) Cardinality

Figure 9: Average run-time, number of iterations performed, and cardinality of returned solution plotted as a function of number of features p ; values of each statistic were averaged across 100 trials. All axes use logarithmic scale.

increases, explains the increase in total run-time of LARS as p increases. Finally, the cardinality of returned discriminant vectors scales similarly for the four proximal gradient methods (PG, PGB, APG, APGB) and LARS. The discriminant vectors returned by ADMM consistently contain fewer nonzero entries than the four other methods, which agrees with the behaviour observed in the Section 3.2.

3.4 Classification of Real-World Data

We performed similar analyses using data sets drawn from the UC Riverside Time-Series Clustering and Classification data repository [10] to verify that the behaviour observed with synthetic data is also observed when classifying real-world data. We applied each of the methods APG, ADMM, SZVD, and LARS to learn classification rules for each of the data sets in the UCR repository with number of training samples n less than the number of predictive features p ; this yielded a collection of 62 data sets to analyze. We omit PG and the backtracking methods from this analysis because our analysis of synthetic data established that these methods are typically less effective than the remaining approaches. We use each remaining sparse discriminant analysis heuristic to obtain $q = K - 1$ sparse discriminant vectors and then perform nearest-centroid classification after projection onto the subspace spanned by these discriminant vectors.

In all experiments, we set $\gamma = 10^{-3}$ and $\mathbf{\Omega}$ to be the $p \times p$ identity matrix $\mathbf{\Omega} = \mathbf{I}$. We choose λ using 10-fold cross validation from the set of potential λ of the form $\bar{\lambda}/2^c$ for $c = 9, 8, 7, \dots, -1, -2, -3$ with $\bar{\lambda}$ defined by (34) to be the value of λ with fewest average number of misclassification errors over training-validation splits amongst all λ which yield discriminant vectors containing at most 30% nonzero entries. We use 10-fold cross validation to select the maximum cardinality in the LARS algorithm from 13 equally spaced potential values from $0.025qp$ to $0.5qp$. We terminate each proximal algorithm in the inner loop after 2000 iterations or a 10^{-7} suboptimal solution is obtained and the outer loop is stopped after a maximum number of 250 iterations or a 10^{-5} suboptimal solution has been found. The augmented Lagrangian parameter $\mu = 2$ was used in ADMM. We use the augmented Lagrangian parameter $\beta = 5$ and choose the regularization parameter γ in SZVD from the exponentially spaced grid $\bar{\gamma}/2^c$ for $c = 9, 8, \dots, -2, -3$ with $\bar{\gamma}$ defined by (35) using 10-fold cross-validation; γ is chosen to minimize average validation set misclassification error amongst all sets of discriminant vectors with at most 30% nonzero entries. We stop SZVD after a maximum of 250 iterations or a solution satisfying the stopping tolerance of 10^{-5} is obtained. These parameters were chosen experimentally to ensure that all methods converge for each data set in the benchmarking set. It is likely that some variation in performance of the heuristics across data sets could be eliminated by more carefully tuning parameters for each individual data set. We assigned the same choice of parameters for each experiment to avoid having to tune parameters separately for all 62 data sets. All simulations were conducted using R version 3.5.0 using the UAHPC; our proximal methods for sparse optimal scoring are implemented in R as the package **accSDA** (see [12]).

3.4.1 Discussion

To empirically test accuracy of each proposed classification heuristic, we calculated the out-of-sample misclassification rate for each data set in the UCR repository. We include baseline accuracies based on the classification results of 1-Nearest Neighbour classifiers: each test observation was assigned the class label of its nearest training observation. As a measure of similarity, we use both *Euclidean distance* (ED), *dynamic time warping distance* with fixed warping window width $w = 100$ (DTW) and learned window width (DTWL). The out-of-sample misclassification rate for each of these classifiers is provided by the UCR Time Series Archive; we direct the reader to refer to [9, Section II] for further details.

For each ordered pair of classification heuristics, we perform a one-sided Wilcoxon signed-rank test. Specifically, for each pair of classification heuristics (i, j) we perform a one-sided Wilcoxon test to test the null hypothesis $H_0 : \text{err}(i) = \text{err}(j)$ against the alternative hypothesis $H_a : \text{err}(i) < \text{err}(j)$, where $\text{err}(x)$ denotes the population average misclassification error rate for classifier x . Figure 12 provides a box plot visualizing average misclassification rate for each method, as well as a table of p -values for the one-sided Wilcoxon significance tests. We observe no significant difference between our APG and ADMM classifiers and all methods except for dynamic time warping with learned window width (DTWL); we obtain p -values of 0.0308 and 0.0478 when testing $H_a : \text{err}(\text{DTWL}) < \text{err}(\text{APG})$ and $H_a : \text{err}(\text{DTWL}) < \text{err}(\text{ADMM})$, respectively, and no other p -values less than 0.05 in any hypothesis tests involving APG and ADMM. We

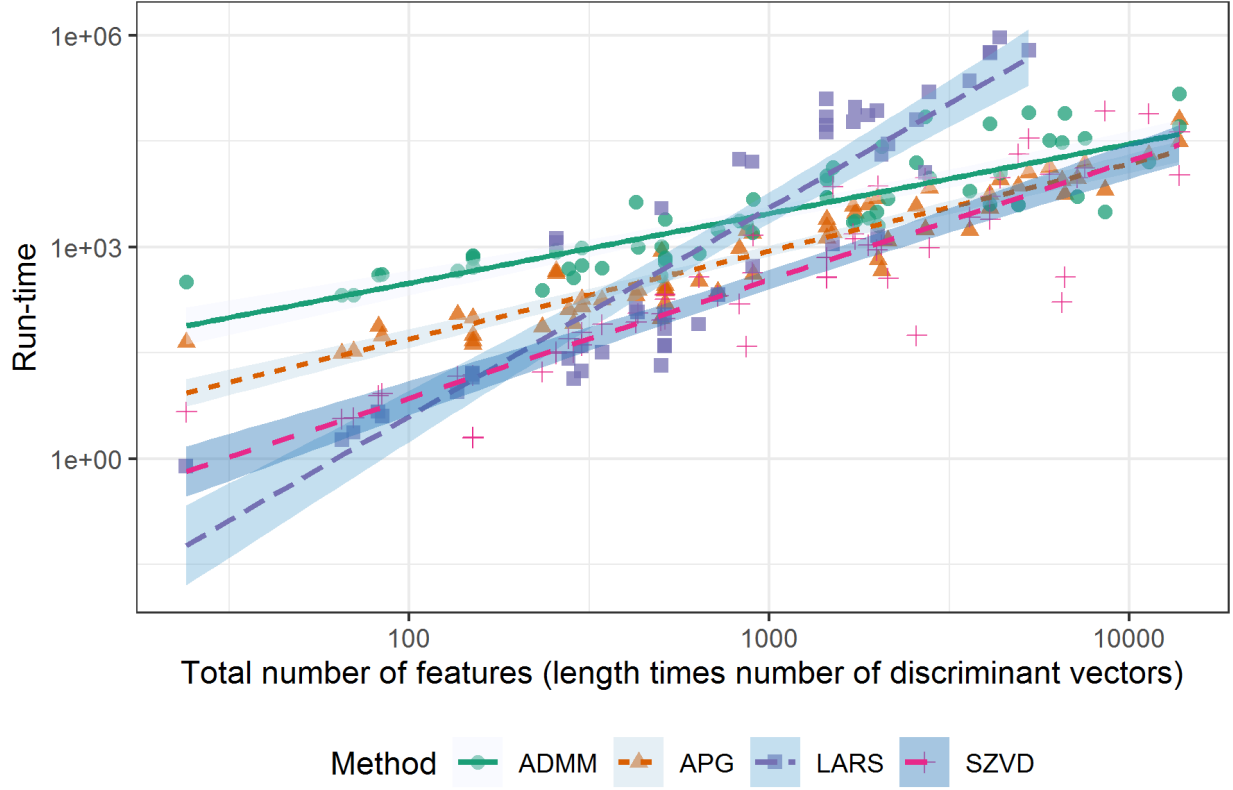
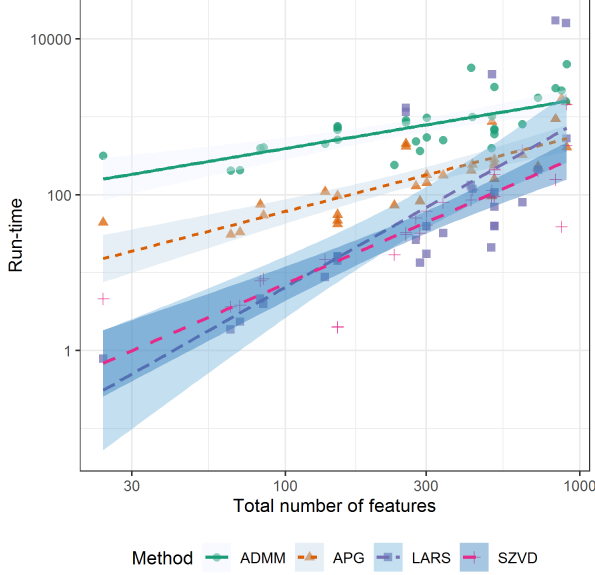


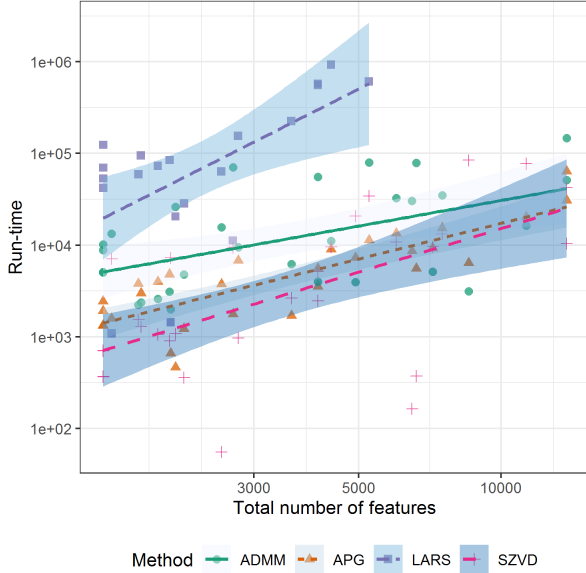
Figure 10: Plot of run-time of each sparse discriminant heuristic as a function of the total number of predictive features (p times number of discriminant vectors). We also fit a line to the set of run-times for each method and 95%-confidence intervals for these linear models. Both axes use logarithmic scale. Experiments where LARS failed to terminate within 11 days were omitted.



(a) Run-times for Small-scale Data

	APG	ADMM	SZVD	LARS
LARS	7.13e-03	5.07e-05	6.83e-01	5.03e-01
SZVD	2.12e-04	1.42e-13	5.03e-01	3.22e-01
ADMM	1.00e+00	5.03e-01	1.00e+00	1.00e+00
APG	5.03e-01	2.80e-08	1.00e+00	9.93e-01

(b) Hypothesis Tests for Small-scale Data

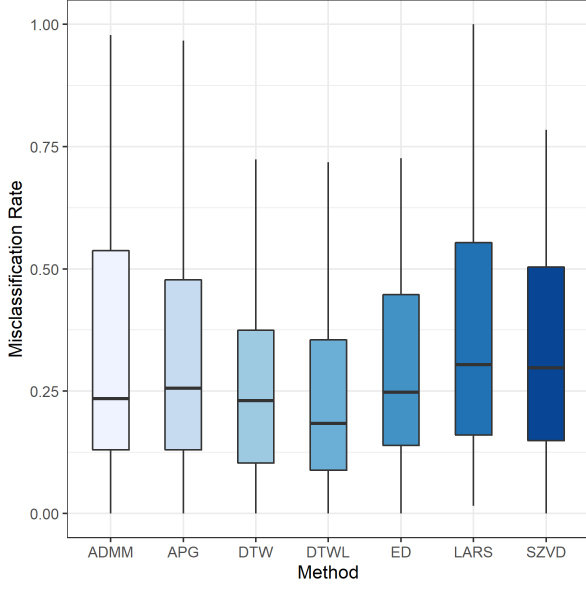


(c) Run-times for Large-scale Data

	APG	ADMM	SZVD	LARS
LARS	1.00e+00	1.00e+00	1.00e+00	5.03e-01
SZVD	1.79e-01	2.27e-03	5.03e-01	4.67e-09
ADMM	9.97e-01	5.03e-01	9.98e-01	5.64e-07
APG	5.03e-01	2.88e-03	8.25e-01	7.22e-09

(d) Hypothesis Tests for Large-scale Data

Figure 11: Plots of run-time for small-scale (total number of features less than 1000) and larger-scale data (total number of features exceeding 1000) included in the UCR benchmarking repository. We also include the results of from one-sided Wilcoxon signed-rank tests comparing computational efficiency of each pair of sparse discriminant analysis heuristics for each subset of benchmarking data. The (i, j) box represents the observed p -value for the test with null hypothesis $H_0 : \text{time}(i) \geq \text{time}(j)$ and alternative hypothesis $H_a : \text{time}(i) < \text{time}(j)$ where $\text{time}(x)$ denotes the expected total run-time of heuristic x on a given data set; darker colors correspond to smaller p -values or higher significance. The maximum amount of time (11 days or 950400 seconds) was used as run-time for LARS for in the Wilcoxon signed-rank tests if LARS failed to terminate within 11 days.

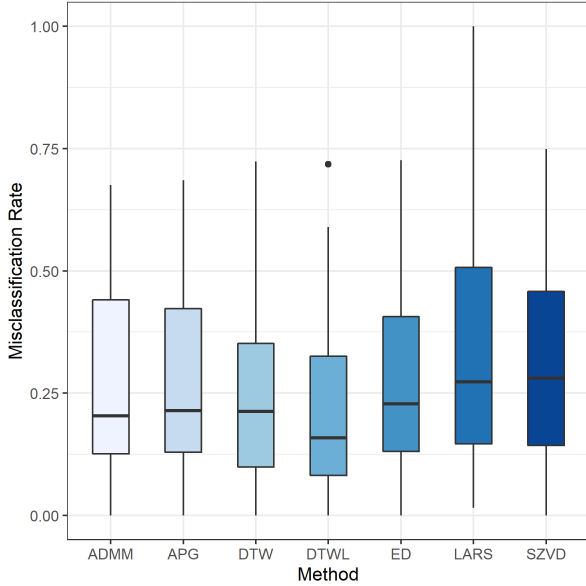


(a) Misclassification Rate

DTWL	3.08e-02	4.78e-02	6.06e-03	1.54e-03	2.70e-02	1.64e-01	5.01e-01
DTW	1.36e-01	1.79e-01	2.78e-02	1.02e-02	1.67e-01	5.01e-01	8.37e-01
ED	4.59e-01	4.89e-01	1.47e-01	7.01e-02	5.01e-01	8.34e-01	9.73e-01
LARS	9.21e-01	9.36e-01	7.52e-01	5.01e-01	9.31e-01	9.90e-01	9.98e-01
SZVD	7.51e-01	7.87e-01	5.01e-01	2.50e-01	8.54e-01	9.73e-01	9.94e-01
ADMM	4.82e-01	5.01e-01	2.14e-01	6.49e-02	5.13e-01	8.22e-01	9.53e-01
APG	5.01e-01	5.20e-01	2.51e-01	8.00e-02	5.43e-01	8.65e-01	9.70e-01
	APG	ADMM	SZVD	LARS	ED	DTW	DTWL

(b) Results of Hypothesis Tests for Accuracy

Figure 12: Box plots of out-of-sample misclassification rates. We also include box plots for misclassification rate for nearest neighbor classification using Euclidean distance (ED) and Dynamic Time Warping distance with fixed warping constraint parameter $w = 100$ (DTW), and learned w (DTWL). We also plot results of one-sided Wilcoxon signed-rank tests for misclassification rate. The (i, j) box represents the observed p -value for the test with null hypothesis $H_0 : \text{err}(i) \geq \text{err}(j)$ and alternative hypothesis $H_a : \text{err}(i) < \text{err}(j)$ where $\text{err}(x)$ denotes the expected fraction of misclassified test observations by classification heuristic x .



(a) Misclassification Rate with Data Sets Omitted

DTWL	6.37e-02	1.05e-01	1.22e-02	2.75e-03	2.91e-02	1.66e-01	5.01e-01
DTW	2.24e-01	3.04e-01	4.46e-02	1.59e-02	1.78e-01	5.01e-01	8.36e-01
ED	6.33e-01	6.72e-01	2.26e-01	1.02e-01	5.01e-01	8.23e-01	9.71e-01
LARS	9.36e-01	9.51e-01	7.24e-01	5.01e-01	8.99e-01	9.84e-01	9.97e-01
SZVD	8.26e-01	8.66e-01	5.01e-01	2.78e-01	7.75e-01	9.56e-01	9.88e-01
ADMM	4.76e-01	5.01e-01	1.35e-01	4.92e-02	3.30e-01	6.98e-01	8.96e-01
APG	5.01e-01	5.27e-01	1.75e-01	6.44e-02	3.69e-01	7.78e-01	9.37e-01
	APG	ADMM	SZVD	LARS	ED	DTW	DTWL

(b) Results of Hypothesis Tests for Accuracy with Data Sets Omitted

Figure 13: Box plots and attained significance/ p -values of out-of-sample misclassification rates with data sets with error at least 70% omitted. Here, we observe no significance difference in classification error (p -value less than 0.05) between APG/ADMM classifiers and DTWL.

do see modest evidence that APG and ADMM are, on average, more accurate than the LARS classifier (p -values 0.08 and 0.0649, respectively). On the other hand, the results of these hypothesis tests suggests a significant improvement in accuracy when using the DTWL classifier over all classifiers except the DTW classifier.

The observed differences between the accuracy of nearest neighbours classifiers, particularly those using dynamic time warping distances, and SOS classifiers can be partially explained by the extremely poor accuracy of SOS classifiers for a small number of data sets. Linear discriminant analysis-based classifiers are only applicable under the assumption that data is linearly separable following projection onto a lower dimensional subspace. The poor accuracy of the SOS classifiers suggest that this linear separability assumption is not satisfied by this subset of the benchmarking repository. If we omit the six data sets in the UCR repository for which the APG classifier yields a misclassification rate of at least 70%, we obtain the average misclassification rates and attained significance visualized in Figure 13. After modifying the benchmarking data set in this way, we observe no significant difference between the APG and ADMM classifiers and the nearest neighbour classifier DTWL at a significance level of $p < 0.05$.

In terms of computational complexity, we can observe two general trends: LARS is consistently more efficient than APG and ADMM when the total number of predictor variables, qp , is small ($qp < 1000$), and APG/ADMM are significantly more efficient than LARS when the number of features is moderate to large ($qp \geq 1000$). Figure 10 plots the total run-time of each sparse discriminant heuristic (including training of parameters by cross-validation), along with linear models fit to observed run-times. There are clear bifurcation points between $500 < qp < 1000$, where the linear models for run-time of APG and ADMM cross that of LARS. To investigate this phenomena further, we isolated run-times for data sets with $qp < 1000$ and $qp \geq 1000$ and performed one-sided Wilcoxon tests for the null hypothesis $H_0 : \text{time}(i) = \text{time}(j)$ and alternative hypothesis $H_a : \text{time}(i) < \text{time}(j)$ under both settings. The results of these significance tests can be found in Figure 11, along with plots of run-times. These tests strongly suggest that LARS is significantly more efficient than both ADMM and APG ($p < 0.001$ in both cases) when the total number of predictor variables is less than 1000. On the other hand, both APG and ADMM require significantly less computation than LARS when the total number of predictor variables is greater than 1000; we observe p values on the order of 10^{-9} and 10^{-7} when testing $\text{time}(\text{APG}) < \text{time}(\text{LARS})$ and $\text{time}(\text{ADMM}) < \text{time}(\text{LARS})$ respectively. In fact, there were 12 different data sets within the UCR Time Series Archive, for which Algorithm 1 failed terminate within 11 days (set as our maximum computation time limit) when using LARS to solve subproblem (13) and 10-fold cross-validation to choose sparsity level; Alg. 1 using APG or ADMM terminated within a few hours for each of these data sets. This scaling largely agrees with that observed for synthetic data in Section 3.3.

We should note that we do not include nearest neighbor classifiers in this discussion of computational efficiency, although we used these methods to obtain a baseline accuracy to benchmark our proposed methods against. The accuracies of these classifiers were provided with the UCR repository and, thus, did not require retraining of the classifiers. Naive implementation of nearest neighbours methods requires at least $\mathcal{O}(n^2p)$ operations to calculate pairwise Euclidean distances and $\mathcal{O}(n^2p^2)$ flops to calculate DTW distances (plus additional operations for training the window width w); optimized methods for DTW reduce this computational cost to $\mathcal{O}(n^2p)$ flops. We, therefore, expect our methods to scale at least as well as these nearest neighbours methods.

3.5 Multispectral X-ray images and Ω of varying rank

To demonstrate the improvement in run-time obtained by using a low-rank Ω in the elastic-net penalty, we perform pixelwise classification on multispectral X-ray images, as presented in [13]. The multispectral X-ray images are scans of food items, where each pixel contains 128 measurements (channels) corresponding to attenuation of X-rays emitted at different wavelengths (see Figure 14). The measurements in each pixel thus give us a profile for the material positioned at that pixel’s location (see Figure 15).

We start by preprocessing the scans as in [13] in order to remove scanning artifacts and normalize the intensities between scans. We scale the measurements in each pixel by the 95% quantile of the corresponding 128 measurements instead of the maximum. This scaling approach is more robust in the sense that it is less sensitive to outliers compared to using the maximum. We create our training data by manually selecting rectangular patches from six scans. We have three classes, namely *background*, *minced meat* and *foreign*

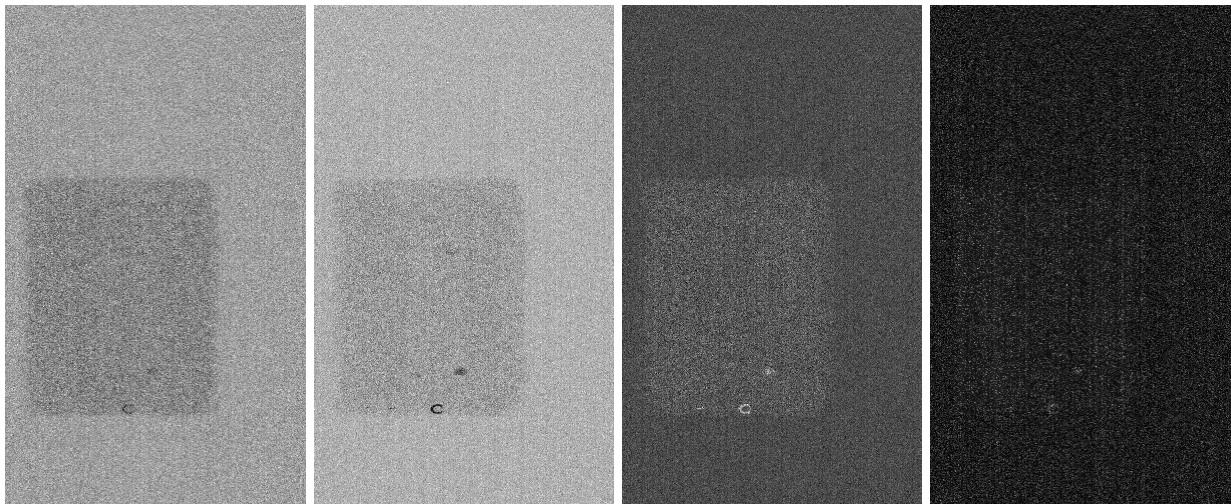


Figure 14: Grayscale images of different channels from a minced meat sample generated with a multispectral X-ray scanner after all preprocessing. From left to right are channels 2, 20, 50 and 100. The contrast decreases the higher we go in the channels and the variation in the measurements increases. Some foreign objects can be seen as small black dots.

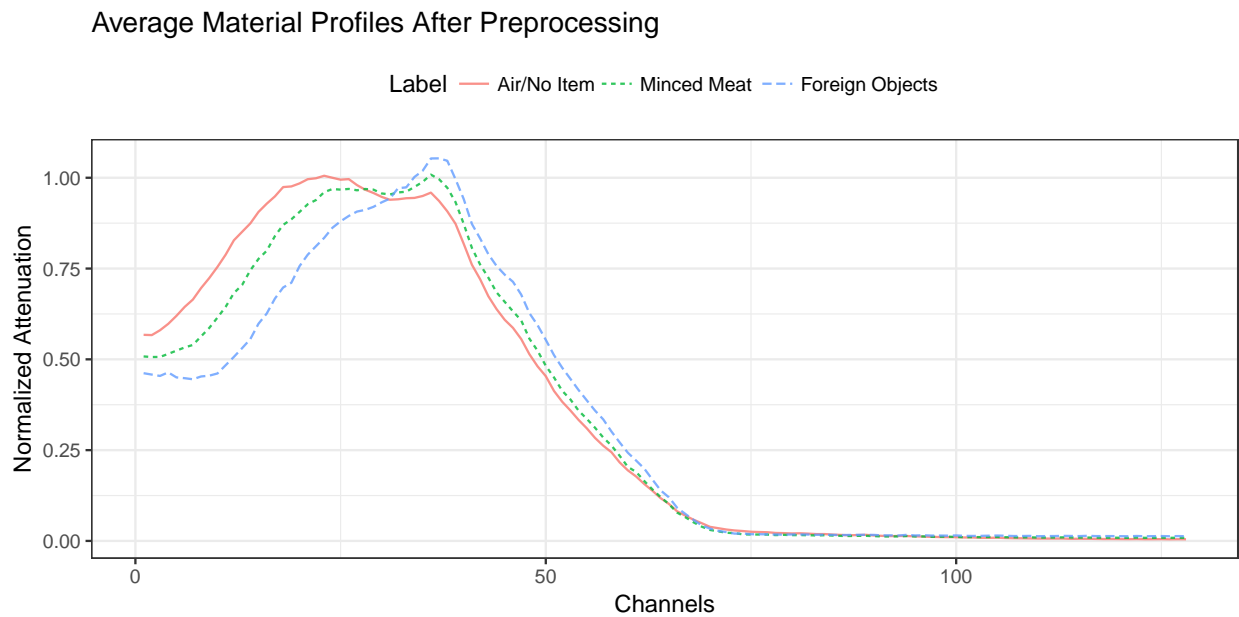


Figure 15: Profiles of materials seen in Figure 14 over the 128 channels. The profile for each type of material, displayed here, is averaged over 500 pixels.

objects. We further subsample the observations to have balanced number of observations, where the class *foreign objects* was under represented. In the end we have 521 observations per class, where each observation corresponds to a single pixel. This data was used to generate Figure 15. For training we use 100 samples per class, and the rest is allocated to a final test set. This process yields 128 variables per observation, but in order to get more spatially consistent classification, we also include data from the pixels located above, to the right, below and to the left of the observed pixel. Thus we have $p = 5 \cdot 128 = 640$ variables per observation. The measurements corresponding to our observation are thus indexed according to spatial and spectral position, i.e., observation \mathbf{x}_i has measurements x_{ijk} , where $j \in \{0, 1, 2, 3, 4\}$ indicates which pixel the measurement belongs to (*center, above, right, bottom, left*), and $k \in \{1, 2, \dots, 128\}$ indicates which channel.

We can impose priors according to these relationships of the measurements in the $\mathbf{\Omega}$ regularization matrix. We assume that the errors should vary smoothly in space and thus impose a Matérn covariance structure on $\mathbf{\Omega}^{-1}$ [29]:

$$C_\nu(d) = \sigma^2 \frac{2^{1-\nu}}{\Gamma(\nu)} \left(\sqrt{2\nu} \frac{d}{\rho} \right)^\nu K_\nu \left(\sqrt{2\nu} \frac{d}{\rho} \right). \quad (37)$$

The Matérn covariance structure (37) is governed by the distance d between measurements. In (37), Γ refers to the gamma function and K_ν is the modified Bessel function of the second kind. For this example we assume that all parameters are 1, except that ν is 0.5. We further assume that the distance between measurements x_{ijk} and $x_{ij'k'}$ from observation i is the Euclidean distance between the points (x_j, y_j, z_k) and $(x_{j'}, y_{j'}, z_{k'})$, where $x_j, y_j, x_{j'}, y_{j'} \in \{-1, 0, 1\}$ and $z_k, z_{k'} \in \{1, 2, \dots, 128\}$. The distance is thus the same as in the image grid (center, top, bottom, left, right pixel location), and z -dimension corresponds to the channel.

We use a stopping tolerance of 10^{-5} and a maximum of 1000 iterations for the inner loop using the accelerated proximal algorithm, and a stopping tolerance of 10^{-4} and maximum 1000 iterations for the outer block-coordinate loop. The regularization parameter for the l_1 -norm is selected as $\lambda = 10^{-3}$ and $\gamma = 10^{-1}$ for the Tikhonov regularizer. We present the run-time for varying r in Figure 16 and the accuracy with respect to varying r in Figure 17. There is a clear linear trend in rank r for the increase in run-time; this agrees with the analysis of Section 2.4. We also estimate the accuracy for a identity regularization matrix, i.e., $\mathbf{\Omega} = \mathbf{I}$, with the same regularization parameters γ and λ and achieve accuracy of 0.948, which is approximately the same accuracy as when using $\mathbf{\Omega}^{400}$. To demonstrate the effect that the rank of $\mathbf{\Omega}$ has on computational complexity, we obtain the singular value decomposition of $\mathbf{\Omega} = \sum_{i=1}^p \sigma_i \mathbf{u}_i \mathbf{v}_i^T$, and construct a low-rank approximation to $\mathbf{\Omega}$ using the first r singular vectors and singular values: $\mathbf{\Omega}^r = \sum_{i=1}^r \sigma_i \mathbf{u}_i \mathbf{v}_i^T$. We supplied the same parameters to the function `sda` from the library `sparseLDA`; `sda` required 267 seconds to run and achieved an accuracy of 0.949. The maximum accuracy is achieved with the full regularization matrix, which is 0.957.

3.6 Summary

Our proposed proximal methods for sparse discriminant analysis provide a decrease in classification error over the existing LARS approach in almost all experiments. Moreover, we see a significant improvement in terms of computational resources used by the accelerated proximal gradient method (APG and APGB) and alternating direction method of multipliers (ADMM) over LARS for all medium to large-scale problem instances, i.e., when the number of predictor variables p exceeds 1000, without significant loss of classification accuracy when compared to standard nearest neighbours classifiers (ED, DTW); we remind the reader that SOS with APG and ADMM does not match the classification accuracy of the nearest neighbour classifier using dynamic time warping distance with learned window width (DTWL) due to poor classification performance of SDA for a small number of data sets for which SDA does not seem applicable, and that our methods are more efficient than DTWL, offer an element of feature selection via sparsity, and are amenable to learning tasks other than classification as a general dimension reduction tool. We should note that this agrees with the theoretical estimates of computational cost of these methods given in Section 2.4 and Appendix A. Specifically, both APG and ADMM converge linearly with per-iteration complexity on the order of $\mathcal{O}(p)$ floating point operations per-iteration, which leads to overall computation time, as measured in floating point operations, to be far less than the $\mathcal{O}(p^3)$ flops of the classical LARS method. In our experiments, the decrease in run-time is most significant when p is large, where the cost of $\mathcal{O}(p^3)$ flops for LARS becomes prohibitive. For example, SDA fails to terminate within 11 days when used to classify several large-scale

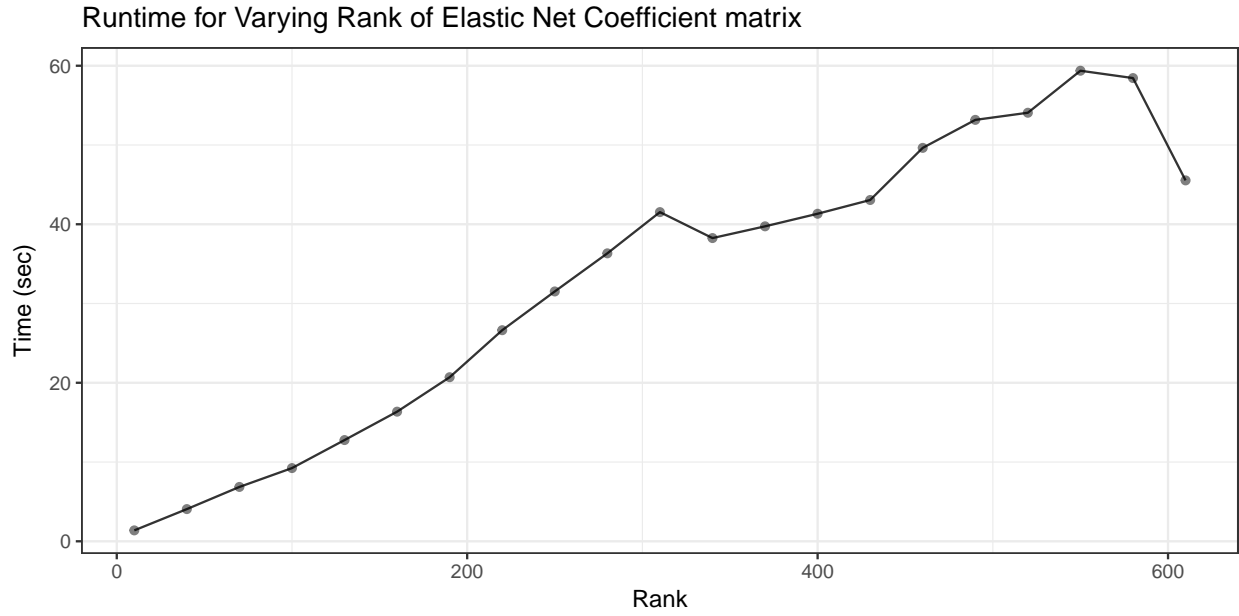


Figure 16: run-time as function of $\text{rank}(\mathbf{\Omega})$. The run-time also includes the creation of the low-rank approximated $\mathbf{\Omega}$ matrix.

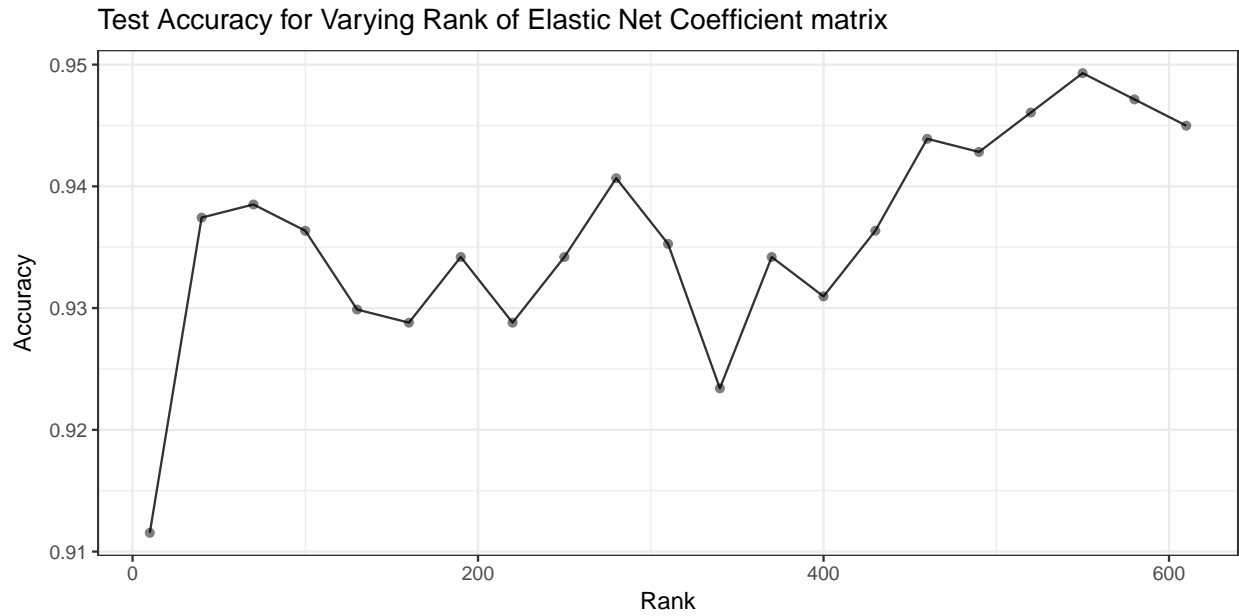


Figure 17: Test accuracy as function of $\text{rank}(\mathbf{\Omega})$

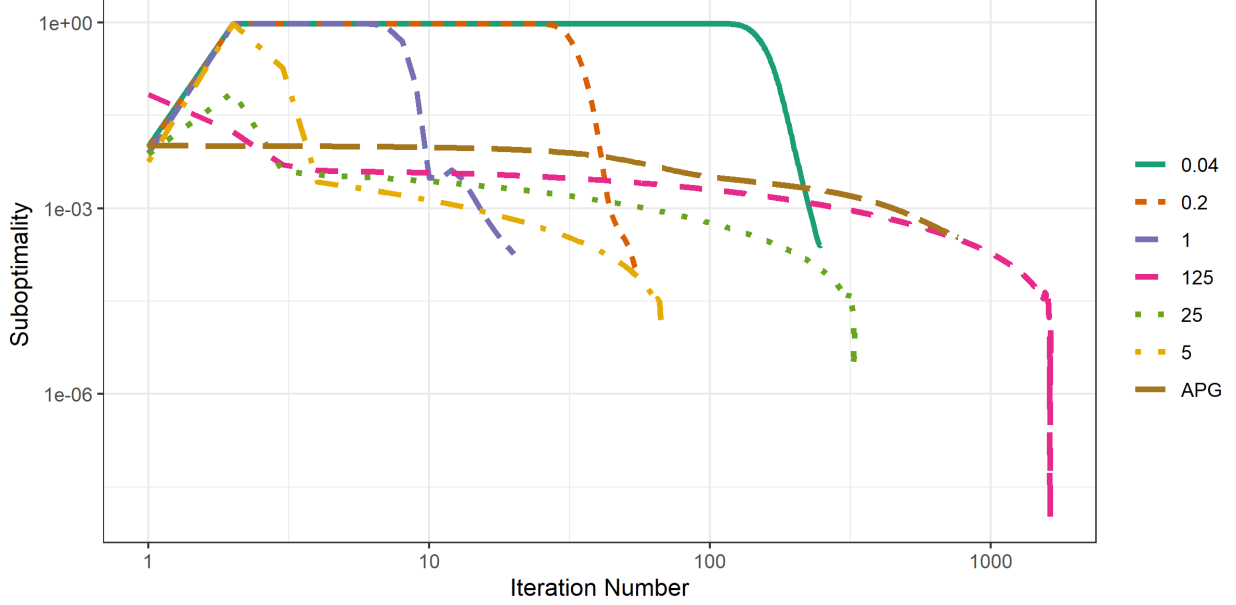


Figure 18: Difference of objective value and optimal value of each iterate averaged across 100 Gaussian data sets. We note that ADMM converges in fewer iterations than APG for all choices of μ except $\mu = 125$.

benchmarking data sets from the UC Riverside repository with LARS used to solve (13) and 10-fold cross-validation; SDA with APG and ADMM used to solve (13) complete this classification task within a few minutes for each of these data sets. It is important to note that the slow convergence of the proximal gradient method (PG/PGB) without acceleration yields significantly longer run-times despite the decreased per-iteration cost. Finally, we note that there appears to be limited benefit from the use of backtracking line search, when compared to a constant step size given by the Frobenius norm estimate $\|\mathbf{A}\|_F$ of the Lipschitz constant. Specifically, the results of these experiments indicate that using a constant step length yields similar classification performance to the backtracking approach, but without a significant increase in run-time due to repeated calculation of ∇f .

3.6.1 Comparison of ADMM and APG

The results of our empirical analysis suggest that the use of either APG and ADMM to solve (13) yields a significant improvement over the classical LARS-EN heuristic. However, which of these two methods is most efficient varies under different experimental conditions. Specifically, APG generally requires less overall run-time than ADMM when analyzing the synthetic data considered in Section 3.1 and data sets from the UCR benchmarking repository considered in Section 3.4. On the other hand, ADMM tends to converge more quickly and require less computation than APG in our convergence tests (Sect. 3.2) and scaling tests (Sect. 3.3). This suggests that performance of the ADMM heuristic is sensitive to the choice of the augmented Lagrangian parameter μ , as this is the only parameter that varies between these different analyses.

We performed the following analysis to further illustrate this sensitivity to the choice of μ . We generated 100 different data sets containing $n = 200$ training observations sampled from each of the $p = 2000$ dimensional Gaussian distributions $N(\boldsymbol{\mu}_1, \boldsymbol{\Sigma})$ and $N(\boldsymbol{\mu}_2, \boldsymbol{\Sigma})$ as in Section 3.2. For each problem instance, we (approximately) solved (2) using APG and ADMM with $\mu \in \{1/25, 1/5, 1, 5, 25, 125\}$ to solve (13). We set $\gamma = 10^{-3}$, $\boldsymbol{\Omega} = \mathbf{I}$, $\lambda = 0.05\bar{\lambda}$ and terminate APG or ADMM if their respective stopping criteria are met with tolerance $10^{-4}/\sqrt{p}$. For each data set, we record the objective function value of (13) at each iteration, as well as cardinality of the obtained discriminant vector, number of iterations performed before termination, total run-time, and out-of-sample classification accuracy for a testing set of 200 observations drawn from each of $N(\boldsymbol{\mu}_1, \boldsymbol{\Sigma})$ and $N(\boldsymbol{\mu}_2, \boldsymbol{\Sigma})$. Note that we are essentially repeating our analysis from Section 3.2, except this time we focus only APG and ADMM under varying choices of μ .

Method	Cardinality	Run-Time	Number of Iterations
APG	536.1 (92)	2.902 (0.531)	766 (136.9)
$\mu = 1/25$	280.4 (7.2)	0.941 (0.066)	248.7 (3.4)
$\mu = 1/5$	291.3 (8.7)	0.29 (0.022)	55.9 (0.7)
$\mu = 1$	410.1 (12.7)	0.171 (0.013)	20.7 (0.6)
$\mu = 5$	426.6 (12.8)	0.33 (0.026)	67.5 (2.9)
$\mu = 25$	428.4 (12.3)	1.212 (0.1)	328.6 (14.6)
$\mu = 125$	428.7 (12.3)	5.63 (0.475)	1639.7 (73.4)

Table 2: Average number of nonzero entries (of $p = 2000$), average run-time, and average number of iterations performed before termination, with standard deviation in parentheses. We see that ADMM yields sparser solutions than APG for all choices of μ and is more efficient than APG for all μ except $\mu = 125$, in terms of both total run time and number of iterations performed. All methods achieved 100% out-of-sample classification rate for all 100 training/testing data sets.

Figure 18 and Table 2 summarize the results of this analysis. Recall that ADMM follows an (approximate) dual ascent applied to the dual functional of (25). The augmented Lagrangian parameter μ controls emphasis between the objective function of (25) and the quadratic penalty function $\|\mathbf{x} - \mathbf{y}\|_2^2$. When μ is large, iterations of ADMM generally decrease disagreement between \mathbf{x} and \mathbf{y} while making only modest decreases, or even increases, in the objective $\frac{1}{2}\mathbf{x}^T \mathbf{A} \mathbf{x} + \mathbf{d}^T \mathbf{x} + \lambda \|\mathbf{y}\|_1$; this corresponds to the slow convergence observed when $\mu = 125$. On the other hand, when μ is very small, we have significant decrease in the objective function each iteration, but many iterations are required before disagreement between \mathbf{x} and \mathbf{y} is small. We observe a two-stage phenomena in our experiments, where early iterations of ADMM feature slow decrease or increase in objective value while the gap between \mathbf{x} and \mathbf{y} decreases, followed by sharp descent in objective value; this initial period is longest when μ is small. This provides empirical evidence that we need to carefully choose the penalty parameter μ in order to optimize convergence of our ADMM heuristic, and partially explains the gap in efficiency between APG and ADMM observed in our experiments. Specifically, ADMM is more efficient than APG only if a suitable choice of μ is used; if we do not carefully tune this penalty parameter, APG can be significantly more efficient than ADMM, as observed in our analysis of benchmarking data from the UCR repository, where we used the same value of μ in all analyses.

4 Conclusion

We have proposed new algorithms for solving the sparse optimal scoring problem for high-dimensional linear discriminant analysis based on block coordinate descent and proximal operator evaluations. We observe that these algorithms provide significant improvement over existing approaches for solving the SOS problem in terms of efficiency and scalability. These improvements are most acute in the case that specially structured Tikhonov regularization is employed in the SOS formulation; for example, the computational resources required for each iteration scales linearly with the dimension of the data if either a diagonal or low-rank matrix is used. Moreover, we establish that any convergent subsequence of iterates generated by one of our algorithms converges to a stationary point. Finally, numerical simulation establishes that our approach provides an improvement over existing methods for sparse discriminant analysis in terms of both quality of solution and run-time.

These results present several exciting avenues for future research. Although we focus primarily on the solution of the optimal scoring problem under regularization in the form of a generalized elastic net penalty, our approach should translate immediately to formulations with any nonsmooth convex penalty function. That is, the framework provided by Algorithm 1 can be applied to solve the SOS problem (2) obtained by applying an arbitrary convex penalty to the objective of the optimal scoring problem (1). The resulting optimization problem can be approximately solved by alternately minimizing with respect to the score vector $\boldsymbol{\theta}$ using the formula (4) and with respect to the discriminant vector $\boldsymbol{\beta}$ by solving a modified version of (13). The proximal methods outlined in this paper can be applied to minimize with respect to $\boldsymbol{\beta}$ if the regularization function is convex, however it is unlikely that the computational resources necessary for

this minimization will scale as favorably as with the generalized elastic net penalty. On the other hand, the convergence analysis presented in Section 2.5 extends immediately to this more general framework. Of particular interest is the modification of this approach to provide means of learning discriminant vectors for data containing ordinal labels, data containing corrupted or missing observations, and semi-supervised settings.

Finally, the results found in Section 2.5, as well as Appendices B and C establish that any convergent subsequence of iterates generated by our block coordinate descent approach must converge to a stationary point. However, it is still unclear when this sequence of iterates is convergent, or at what rate these subsequences converge; further study is required to better understand the convergence properties of these algorithms. Similarly, despite the empirical evidence provided in Section 3, it is unknown what conditions ensure that data is classifiable using sparse optimal scoring and, more generally, linear discriminant analysis. Extensive consistency analysis is needed to determine theoretical error rates for distinguishing random variables drawn from distinct distributions.

4.1 Acknowledgements

We are grateful to Mingyi Hong for his helpful comments and suggestions, and to the anonymous reviewers, whose suggestions significantly improved this manuscript. B. Ames was supported in part by National Science Foundation Grant #20212554, University of Alabama Research Grants RG14678 and RG14838, and a UA Cyberseed Grant. G. Einarsson’s PhD scholarship was funded by the Lundbeck foundation and the Technical University of Denmark. S. Atkins was part of the University Scholars Program at the University of Alabama and received a graduate student fellowship funded by the University of Florida while this research was conducted.

References

- [1] Allen-Zhu, Z., Orecchia, L.: Linear coupling: An ultimate unification of gradient and mirror descent (2014)
- [2] Ames, B., Hong, M.: Alternating direction method of multipliers for penalized zero-variance discriminant analysis. *Computational Optimization and Applications* **64**(3), 725–754 (2016). DOI 10.1007/s10589-016-9828-y
- [3] Beck, A.: First-order methods in optimization, vol. 25. SIAM (2017)
- [4] Beck, A., Teboulle, M.: A fast iterative shrinkage-thresholding algorithm for linear inverse problems. *SIAM journal on imaging sciences* **2**(1), 183–202 (2009). DOI 10.1137/080716542
- [5] Boyd, S., Parikh, N., Chu, E., Peleato, B., Eckstein, J.: Distributed optimization and statistical learning via the alternating direction method of multipliers. *Foundations and Trends® in Machine Learning* **3**(1), 1–122 (2011). DOI 10.1561/22000000016
- [6] Bubeck, S., Lee, Y.T., Singh, M.: A geometric alternative to Nesterov’s accelerated gradient descent (2015)
- [7] Cai, T., Liu, W.: A direct estimation approach to sparse linear discriminant analysis. *Journal of the American Statistical Association* **106**(496), 1566–1577 (2011). DOI 10.1198/jasa.2011.tm11199
- [8] Clemmensen, L., Hastie, T., Witten, D., Ersbøll, B.: Sparse discriminant analysis. *Technometrics* **53**(4), 406–413 (2011). DOI 10.1198/TECH.2011.08118
- [9] Dau, H.A., Bagnall, A., Kamgar, K., Yeh, C.C.M., Zhu, Y., Gharghabi, S., Ratanamahatana, C.A., Keogh, E.: The ucr time series archive (2019)
- [10] Dau, H.A., Keogh, E., Kamgar, K., Yeh, C.C.M., Zhu, Y., Gharghabi, S., Ratanamahatana, C.A., Yanping, Hu, B., Begum, N., Bagnall, A., Mueen, A., Batista, G., Hexagon-ML: The ucr time series classification archive (2018). https://www.cs.ucr.edu/~eamonn/time_series_data_2018/

- [11] Deng, W., Yin, W.: On the global and linear convergence of the generalized alternating direction method of multipliers. *Journal of Scientific Computing* **3**(66), 889–916 (2012). DOI 10.1007/s10915-015-0048-x
- [12] Einarsson, G., Clemmensen, L., Ames, B., Atkins, S.: accsda: Accelerated sparse discriminant analysis (2017). URL <https://cran.r-project.org/web/packages/accSDA/index.html>. Also available at <https://github.com/gumeo/accSDA>
- [13] Einarsson, G., Jensen, J.N., Paulsen, R.R., Einarsdottir, H., Ersbøll, B.K., Dahl, A.B., Christensen, L.B.: Foreign object detection in multispectral x-ray images of food items using sparse discriminant analysis. In: *Scandinavian Conference on Image Analysis*, pp. 350–361. Springer (2017)
- [14] Fan, J., Fan, Y.: High dimensional classification using features annealed independence rules. *Annals of Statistics* **36**(6), 2605–2637 (2008). DOI 10.1214/07-AOS504
- [15] Flammarion, N., Bach, F.: From averaging to acceleration, there is only a step-size (2015)
- [16] Friedman, J., Hastie, T., Tibshirani, R.: Regularization paths for generalized linear models via coordinate descent. *Journal of statistical software* **33**(1), 1 (2010)
- [17] Goldfarb, D., Ma, S., Scheinberg, K.: Fast alternating linearization methods for minimizing the sum of two convex functions. *Mathematical Programming* **141**(1), 349–382 (2013)
- [18] Golub, G.H., Van Loan, C.F.: *Matrix Computations*, 4th edn. The Johns Hopkins University Press, Baltimore (2013)
- [19] Grosenick, L., Greer, S., Knutson, B.: Interpretable classifiers for fmri improve prediction of purchases. *IEEE transactions on neural systems and rehabilitation engineering* **16**(6), 539–548 (2008)
- [20] Hastie, T., Buja, A., Tibshirani, R.: Penalized discriminant analysis. *The Annals of Statistics* pp. 73–102 (1995)
- [21] Hastie, T., Tibshirani, R., Buja, A.: Flexible discriminant analysis by optimal scoring. *Journal of the American Statistical Association* **89**(428), 1255–1270 (1994). DOI 10.2307/2290989
- [22] Hastie, T., Tibshirani, R., Friedman, J.H.: *The Elements of Statistical Learning*, 2nd edn. Springer-Verlag New York, New York (2013)
- [23] Hastie, T., Tibshirani, R., Wainwright, M.: *Statistical Learning with Sparsity: the Lasso and Generalizations*, 1st edn. CRC Press, Boca Raton and London and New York (2012)
- [24] He, B., Yuan, X.: On the $o(1/n)$ convergence rate of the douglas–rachford alternating direction method. *SIAM Journal on Numerical Analysis* **50**(2), 700–709 (2012)
- [25] Lessard, L., Recht, B., Packard, A.: Analysis and design of optimization algorithms via integral quadratic constraints. *SIAM Journal on Optimization* **26**(1), 57–95 (2016). DOI 10.1137/15M1009597
- [26] Ma, Q., Yuan, M., Zou, H.: A direct approach to sparse discriminant analysis in ultra-high dimensions. *Biometrika* **99**, 29–42 (2012). DOI 10.1093/biomet/asr066
- [27] Mai, Q., Zou, H.: A note on the connection and equivalence of three sparse linear discriminant analysis methods. *Technometrics* **55**(2), 243–246 (2013). DOI 10.1080/00401706.2012.746208
- [28] Mai, Q., Zou, H.: *Multiclass sparse discriminant analysis* (2015)
- [29] Matérn, B.: *Spatial variation*, vol. 36. Springer Science & Business Media (2013)
- [30] Merchante, L.F.S., Grandvalet, Y., Govaert, G.: An efficient approach to sparse linear discriminant analysis. *arXiv preprint arXiv:1206.6472* (2012)
- [31] Nesterov, Y.: A method of solving a convex programming problem with convergence rate $o(1/k^2)$. In: *Soviet Mathematics Doklady*, vol. 27, pp. 372–376 (1983). URL <http://mpawankumar.info/teaching/cdt-big-data/nesterov83.pdf>

- [32] Nesterov, Y.: Smooth minimization of non-smooth functions. *Mathematical programming* **103**(1), 127–152 (2005). DOI 10.1007/s10107-004-0552-5
- [33] Nesterov, Y.: Gradient methods for minimizing composite functions. *Mathematical Programming* **140**(1), 125–161 (2013). DOI 10.1007/s10107-012-0629-5
- [34] Nishihara, R., Lessard, L., Recht, B., Packard, A., Jordan, M.: A general analysis of the convergence of admm. In: *International Conference on Machine Learning*, pp. 343–352. PMLR (2015)
- [35] Nocedal, J., Wright, S.: *Numerical optimization*, 2nd edn. Springer Science & Business Media, New York (2006)
- [36] O’Donoghue, B., Candes, E.: Adaptive restart for accelerated gradient schemes. *Foundations of Computational Mathematics* **15**(3), 715–732 (2015). DOI 10.1007/s10208-013-9150-3
- [37] Parikh, N., Boyd, S.P.: Proximal algorithms. *Foundations and Trends in optimization* **1**(3), 127–239 (2014). DOI 10.1561/24000000003
- [38] Roth, V., Fischer, B.: The group-lasso for generalized linear models: uniqueness of solutions and efficient algorithms. In: *Proceedings of the 25th international conference on Machine learning*, pp. 848–855 (2008)
- [39] Shao, J., Wang, Y., Deng, X., Wang, S.: Sparse linear discriminant analysis by thresholding for high dimensional data. *The Annals of Statistics* **39**(2), 1241–1265 (2011). DOI 10.1214/10-AOS870
- [40] Su, W., Boyd, S., Candes, E.: A differential equation for modeling nesterov’s accelerated gradient method: Theory and insights. In: *Advances in Neural Information Processing Systems*, pp. 2510–2518 (2014)
- [41] Tibshirani, R., Hastie, T., Narasimhan, B., Chu, G.: Class prediction by nearest shrunken centroids, with applications to dna microarrays. *Statistical Science* pp. 104–117 (2003). DOI 10.1214/ss/1056397488
- [42] Tseng, P.: On accelerated proximal gradient methods for convex-concave optimization (2008). URL <http://www.mit.edu/~dimitrib/PTseng/papers/apgm.pdf>
- [43] Witten, D.M., Tibshirani, R.: Penalized classification using Fisher’s linear discriminant. *Journal of the Royal Statistical Society: Series B (Statistical Methodology)* **73**(5), 753–772 (2011). DOI 10.1111/j.1467-9868.2011.00783.x
- [44] Wu, M., Zhang, L., Wang, Z., Christiani, D., Lin, X.: Sparse linear discriminant analysis for simultaneous testing for the significance of a gene set/pathway and gene selection. *Bioinformatics* **25**(9), 1145–1151 (2008). DOI 10.1093/bioinformatics/btp019
- [45] Zou, H., Hastie, T.: Regularization and variable selection via the elastic net. *Journal of the Royal Statistical Society: Series B (Statistical Methodology)* **67**(2), 301–320 (2005). DOI 10.1111/j.1467-9868.2005.00503.x

A Detailed Calculation of Per-Iteration Complexity

The most expensive step of both the proximal gradient method (Algorithm 3) and the accelerated proximal gradient method (Algorithm 4) is the evaluation of the gradient ∇f . Given a vector $\beta \in \mathbf{R}^p$, the gradient at β is given by

$$\nabla f(\beta) = A\beta = 2 \left(X^T X + \gamma \Omega \right) \beta = 2X^T X\beta + 2\gamma\Omega\beta.$$

The product $X^T X\beta$ can be computed using $\mathcal{O}(np)$ floating point operations (flops) by computing $y = X\beta$ and then $X^T y$. On the other hand, the product $\Omega\beta$ requires $\mathcal{O}(p^2)$ flops for unstructured Ω . However, if we use a *structured* regularization parameter Ω we can significantly decrease this computational cost. Consider the following examples:

- Suppose that $\mathbf{\Omega}$ is a diagonal matrix: $\mathbf{\Omega} = \text{Diag}(\mathbf{u})$ for some vector $\mathbf{u} \in \mathbf{R}_+^p$. Then the product $\mathbf{\Omega}\beta$ can be computed using $\mathcal{O}(p)$ flops: $(\mathbf{\Omega}\beta)_i = u_i\beta_i$. Moreover, we can estimate the Lipschitz constant $\|\mathbf{A}\|$ for use in choosing the step size α by $\|\mathbf{A}\| \leq 2\gamma\|\mathbf{\Omega}\| + 2\|\mathbf{X}\|_F^2 = 2\gamma\|\mathbf{u}\|_\infty + 2\|\mathbf{X}\|_F^2$, which requires $\mathcal{O}(np)$ flops, primarily to compute the norm $\|\mathbf{X}\|_F^2$.
- If the use of diagonal $\mathbf{\Omega}$ is inappropriate, we could store $\mathbf{\Omega}$ in factored form $\mathbf{\Omega} = \mathbf{R}\mathbf{R}^T$ where $\mathbf{R} \in \mathbf{R}^{p \times r}$, and r is the rank of $\mathbf{\Omega}$. In this case, we have $\mathbf{\Omega}\beta = \mathbf{R}(\mathbf{R}^T\beta)$, which can be computed at a cost of $\mathcal{O}(rp)$ flops. Thus, if we use a low-rank parameter $\mathbf{\Omega}$, say $r \leq \mathcal{O}(n)$, we can compute the gradient using $\mathcal{O}(np)$ flops. Similarly, we can estimate the step size α using $\|\mathbf{A}\| \leq 2\|\mathbf{R}\|_F^2 + 2\|\mathbf{X}\|_F^2$ (computed at a cost of $\mathcal{O}(rp + np)$ flops).

In either case, using a diagonal $\mathbf{\Omega}$ or low-rank factored $\mathbf{\Omega}$, each iteration of the proximal gradient method or the accelerated proximal gradient method requires $\mathcal{O}(np)$ flops. Similar improvements can be made if $\mathbf{\Omega}$ is tridiagonal, banded, sparse, or otherwise nicely structured.

Similarly, the use of structured $\mathbf{\Omega}$ can lead to significant improvements in computational efficiency in our ADMM algorithm. The main computational bottleneck of this method is the solution of the linear system in the update of \mathbf{x} :

$$(\mu\mathbf{I} + \mathbf{A})\mathbf{x}^{i+1} = \mathbf{d} + \mu\mathbf{y}^i - \mathbf{z}^i.$$

Without taking advantage of the structure of \mathbf{A} , we can solve this system using a Cholesky factorization preprocessing step (at a cost of $\mathcal{O}(p^3)$ flops) and substitution to solve the resulting triangular systems (at a cost of $\mathcal{O}(p^2)$ flops per-iteration). However, we can often use the Sherman-Morrison-Woodbury Lemma to solve this system more efficiently using the structure of \mathbf{A} . Indeed, fix t and let $\mathbf{b} = \mathbf{d} + \mu\mathbf{y}^i - \mathbf{z}^i$. Then we update \mathbf{x} by $\mathbf{x} = (\mu\mathbf{I} + \mathbf{A})^{-1}\mathbf{b}$. If $\mathbf{M} = \mu\mathbf{I} + 2\gamma\mathbf{\Omega}$ then we have

$$\begin{aligned} (\mu\mathbf{I} + \mathbf{A})^{-1} &= (\mu\mathbf{I} + 2\gamma\mathbf{\Omega} + 2\mathbf{X}^T\mathbf{X})^{-1} = (\mathbf{M} + 2\mathbf{X}^T\mathbf{X})^{-1} \\ &= \mathbf{M}^{-1} - 2\mathbf{M}^{-1}\mathbf{X}^T \left(\mathbf{I} + 2\mathbf{X}\mathbf{M}^{-1}\mathbf{X}^T \right)^{-1} \mathbf{X}\mathbf{M}^{-1}. \end{aligned}$$

The matrix $\mathbf{I} + 2\mathbf{X}\mathbf{M}^{-1}\mathbf{X}^T$ is $n \times n$, so we may solve any linear system with this coefficient matrix using $\mathcal{O}(n^3)$ flops; a further $\mathcal{O}(n^2p)$ flops are needed to compute the coefficient matrix if given \mathbf{M}^{-1} . Thus, the main computational burden of this update step is the inversion of the matrix \mathbf{M} . As before, we want to choose $\mathbf{\Omega}$ so that we can exploit its structure. Consider the following cases.

- If $\mathbf{\Omega} = \text{Diag}(\mathbf{u})$ is diagonal, then \mathbf{M} is also diagonal with

$$[\mathbf{M}^{-1}]_{ii} = \frac{1}{\mu + 2\gamma u_i}.$$

Thus, we require $\mathcal{O}(p)$ flops to compute $\mathbf{M}^{-1}\mathbf{v}$ for any vector $\mathbf{v} \in \mathbf{R}^p$.

- On the other hand, if $\mathbf{\Omega} = \mathbf{R}\mathbf{R}^T$, where $\mathbf{R} \in \mathbf{R}^{p \times r}$, then we may use the Sherman-Morrison-Woodbury identity to compute \mathbf{M}^{-1} :

$$\mathbf{M}^{-1} = \frac{1}{\mu}\mathbf{I} - \frac{2\gamma}{\mu^2}\mathbf{R} \left(\mathbf{I} + \frac{2\gamma}{\mu}\mathbf{R}^T\mathbf{R} \right)^{-1} \mathbf{R}^T.$$

Therefore, we can solve any linear system with coefficient matrix \mathbf{M} at a cost of $\mathcal{O}(r^2p)$ flops (for the formation and solution of the system with coefficient matrix $\mathbf{I} + \frac{2\gamma}{\mu}\mathbf{R}^T\mathbf{R}$).

In either case, we never actually compute the matrices \mathbf{M}^{-1} and $(\mu\mathbf{I} + \mathbf{A})^{-1}$ explicitly. Instead, we update \mathbf{x} as the solution of a sequence of linear systems and matrix-vector multiplications, at a total cost of $\mathcal{O}(n^2p)$ flops (in the diagonal case) or $\mathcal{O}((r^2 + n^2)p)$ flops (in the factored case). Thus, if the number of observations n is much smaller than the number of features p , then the per-iteration computation scales roughly linearly with p . Table 3 summarizes these estimates of per-iteration computational costs for each proposed algorithm. Further, we should note that these bounds on per-iteration cost assume that the iterates β and \mathbf{x} are dense; the soft-thresholding step of the proximal gradient algorithm typically induces β containing many zeros, suggesting that further improvements can be made by using sparse arithmetic.

		Diagonal Ω	Rank r Ω	Full rank Ω
Proximal Gradient	∇f	$\mathcal{O}(np)$	$\mathcal{O}(rp + np)$	$\mathcal{O}(p^2)$
	Bound on $\ \mathbf{A}\ $	$\mathcal{O}(np)$	$\mathcal{O}(rp + np)$	$\mathcal{O}(p^2 \log p)$
ADMM	$(\mu \mathbf{I} + \mathbf{A})\mathbf{x} = \mathbf{b}$	$\mathcal{O}(n^3 + n^2p)$	$\mathcal{O}(n^3 + n^2p + r^2p)$	$\mathcal{O}(p^3)$

Table 3: Upper bounds on floating point operation counts for most time consuming steps of each algorithm.

B Proof of Theorem 2.5

We next prove Theorem 2.5, which establishes that Algorithm 1 converges in function value.

Proof: Suppose that, after t iterations, we have iterates $(\boldsymbol{\theta}^i, \boldsymbol{\beta}^i)$ with objective function value $F(\boldsymbol{\theta}^i, \boldsymbol{\beta}^i)$. Recall that we obtain $\boldsymbol{\beta}^{i+1}$ as the solution of (13). Moreover, note that $\boldsymbol{\beta}^i$ is also feasible for (13). This immediately implies that

$$F(\boldsymbol{\theta}^i, \boldsymbol{\beta}^i) \geq F(\boldsymbol{\theta}^i, \boldsymbol{\beta}^{i+1}).$$

On the other hand, $\boldsymbol{\theta}^{i+1}$ is the solution of (3) with $\boldsymbol{\beta} = \boldsymbol{\beta}^{i+1}$. Therefore, we have

$$F(\boldsymbol{\theta}^i, \boldsymbol{\beta}^i) \geq F(\boldsymbol{\theta}^i, \boldsymbol{\beta}^{i+1}) \geq F(\boldsymbol{\theta}^{i+1}, \boldsymbol{\beta}^{i+1}).$$

It follows that the sequence of function values $\{F(\boldsymbol{\theta}^i, \boldsymbol{\beta}^i)\}_{i=1}^\infty$ is nonincreasing. Moreover, the objective function $F(\boldsymbol{\theta}, \boldsymbol{\beta})$ is nonnegative for all $\boldsymbol{\theta}$ and $\boldsymbol{\beta}$. Therefore, $\{F(\boldsymbol{\theta}^i, \boldsymbol{\beta}^i)\}_{i=1}^\infty$ is convergent as a monotonic bounded sequence. ■

C Proof of Theorem 2.6

To prove Theorem 2.6, we first establish the following lemma, which establishes that the limit point $(\boldsymbol{\theta}^*, \boldsymbol{\beta}^*)$ minimizes F with respect to each primal variable with the other fixed; that is, $\boldsymbol{\theta}^*$ minimizes $F(\cdot, \boldsymbol{\beta}^*)$ and $\boldsymbol{\beta}^*$ minimizes $F(\boldsymbol{\theta}^*, \cdot)$.

Lemma C.1 *Let $\{(\boldsymbol{\theta}^i, \boldsymbol{\beta}^i)\}_{i=1}^\infty$ be the sequence of points generated by Algorithm 1. Suppose that $\{(\boldsymbol{\theta}^{t_j}, \boldsymbol{\beta}^{t_j})\}_{j=1}^\infty$ is a convergent subsequence of $\{(\boldsymbol{\theta}^i, \boldsymbol{\beta}^i)\}_{i=1}^\infty$ with limit $(\boldsymbol{\theta}^*, \boldsymbol{\beta}^*)$. Then*

$$F(\boldsymbol{\theta}, \boldsymbol{\beta}^*) \geq F(\boldsymbol{\theta}^*, \boldsymbol{\beta}^*) \tag{38}$$

$$F(\boldsymbol{\theta}^*, \boldsymbol{\beta}) \geq F(\boldsymbol{\theta}^*, \boldsymbol{\beta}^*) \tag{39}$$

for all feasible $\boldsymbol{\theta} \in \mathbf{R}^k$ and $\boldsymbol{\beta} \in \mathbf{R}^p$.

Proof: We first establish (39). Consider $(\boldsymbol{\theta}^{t_j}, \boldsymbol{\beta}^{t_j})$. By our update step for $\boldsymbol{\beta}$, we note that

$$\boldsymbol{\beta}^{t_j} = \arg \min_{\boldsymbol{\beta} \in \mathbf{R}^p} F(\boldsymbol{\theta}^{t_j}, \boldsymbol{\beta}).$$

Thus, for all $j = 1, 2, \dots$, we have $F(\boldsymbol{\theta}^{t_j}, \boldsymbol{\beta}) \geq F(\boldsymbol{\theta}^{t_j}, \boldsymbol{\beta}^{t_j})$ for all $\boldsymbol{\beta} \in \mathbf{R}^p$. Taking the limit as $j \rightarrow \infty$ and using the continuity of F establishes (39).

Next, note that, for every $j = 1, 2, \dots$, we have

$$\begin{aligned} \boldsymbol{\theta}^{t_j+1} &= \arg \min_{\boldsymbol{\theta} \in \mathbf{R}^k} F(\boldsymbol{\theta}, \boldsymbol{\beta}^{t_j}) \\ \text{s.t. } \quad &\boldsymbol{\theta}^T \mathbf{Y}^T \mathbf{Y} \boldsymbol{\theta} = n, \quad \boldsymbol{\theta}^T \mathbf{Y}^T \mathbf{Y} \boldsymbol{\theta}_\ell = 0 \quad \forall \ell < k. \end{aligned}$$

This implies that

$$F(\boldsymbol{\theta}, \boldsymbol{\beta}^{t_j}) \geq F(\boldsymbol{\theta}^{t_j+1}, \boldsymbol{\beta}^{t_j}) \geq F(\boldsymbol{\theta}^{t_j+1}, \boldsymbol{\beta}^{t_j+1}) \geq F(\boldsymbol{\theta}^{t_{j+1}}, \boldsymbol{\beta}^{t_{j+1}})$$

by the monotonicity of the sequence of function values and the fact that $t_j < t_j + 1 \leq t_{j+1}$. Taking the limit as $j \rightarrow \infty$ and using the continuity of F establishes (38). This completes the proof of Lemma C.1. ■

We are now ready to prove Theorem 2.6. **Proof:** of Theorem 2.6 The form of the subdifferential of \mathcal{L} implies that $(\mathbf{g}_\theta, \mathbf{g}_\beta)$ belongs to the subdifferential $\partial\mathcal{L}(\theta, \beta, \psi, \mathbf{v})$ if and only if

$$\mathbf{g}_\theta = 2(1 + \psi)\mathbf{Y}^T\mathbf{Y}\theta - 2\mathbf{Y}^T\mathbf{X}\beta + \mathbf{U}^T\mathbf{v} \quad (40)$$

$$\mathbf{g}_\beta \in 2(\mathbf{X}^T\mathbf{X} + \gamma\mathbf{\Omega})\beta - 2\mathbf{X}^T\mathbf{Y}\theta + \lambda\partial\|\beta\|_1 \quad (41)$$

for all $\mathbf{v} \in \mathbf{R}^{j-1}$ and $\psi \in \mathbf{R}$. It is easy to see from (39) that $\beta^* = \arg \min_{\beta \in \mathbf{R}^p} F(\theta^*, \beta)$. Thus, by the first order necessary conditions for unconstrained convex optimization, we must have

$$\begin{aligned} \mathbf{0} &\in \partial \left(\frac{1}{2}(\beta^*)^T \mathbf{A}\beta^* + \mathbf{d}^T\beta^* + \lambda\|\beta^*\|_1 \right) \\ &= 2(\mathbf{X}^T\mathbf{X} + \gamma\mathbf{\Omega})\beta^* - 2\mathbf{X}^T\mathbf{Y}\theta^* + \lambda\partial\|\beta^*\|_1; \end{aligned} \quad (42)$$

here $\partial\|\beta\|_1$ denotes the subdifferential of the ℓ_1 -norm at the point β .

On the other hand, (38) implies

$$\begin{aligned} \theta^* &= \arg \min_{\theta \in \mathbf{R}^K} \|\mathbf{Y}\theta - \mathbf{X}\beta^*\|^2 \\ \text{s.t. } &\theta^T\mathbf{Y}^T\mathbf{Y}\theta = n, \quad 2\theta^T\mathbf{Y}^T\mathbf{Y}\theta_\ell = 0, \quad \forall \ell < j. \end{aligned} \quad (43)$$

Moreover, the problem (43) satisfies the linear independence constraint qualification. Indeed, the set of active constraint gradients

$\{2\mathbf{Y}^T\mathbf{Y}\theta, 2\mathbf{Y}^T\mathbf{Y}\theta_1, \dots, 2\mathbf{Y}^T\mathbf{Y}\theta_{j-1}\}$ is linearly independent for any feasible $\theta \in \mathbf{R}^K$ by the $\mathbf{Y}^T\mathbf{Y}$ -conjugacy of $\{\theta, \theta_1, \dots, \theta_{j-1}\}$. Therefore, there exist Lagrange multipliers ψ^*, \mathbf{v}^* such that

$$\mathbf{0} = 2(1 + \psi^*)\mathbf{Y}^T\mathbf{Y}\theta^* - 2\mathbf{Y}^T\mathbf{X}\beta^* + \mathbf{U}^T\mathbf{v}^* \quad (44)$$

by the first-order necessary conditions for optimality (see [35, Theorem 12.1]). We see that $\mathbf{0} \in \partial\mathcal{L}(\theta^*, \beta^*, \psi^*, \mathbf{v}^*)$ by combining (42) and (44). This completes the proof. ■